rgs-CaM Detects and Counteracts Viral RNA Silencing Suppressors in Plant Immune Priming

Eun Jin Jeon[a], Kazuki Tadamura[a], Taiki Murakami[a], Jun-ichi Inaba[a], Bo Min Kim[a], Masako Sato[c], Go Atsumi[a], Kazuyuki Kuchitsu[b], Chikara Masuta[a,c], Kenji S. Nakahara[a,c]

Graduate School of Agriculture, Hokkaido University, Sapporo, Hokkaido, Japan[a]; Department of Applied Biological Science, and Research Institute for Science and Technology, Tokyo University of Science, Noda, Chiba, Japan[b]; Research Faculty of Agriculture, Hokkaido University, Sapporo, Hokkaido, Japan[c]

Running title: Receptor and Effector for Plant Immune Priming

Keywords: Systemic acquired resistance, Calmodulin-like protein, RNA silencing suppressor, Cucumber mosaic virus

#Address correspondence to Kenji S. Nakahara, knakahar@res.agr.hokudai.ac.jp

E.J.J. and K.T. contributed equally to this work.

The word count for abstract: 250, and the text: 7411

ABSTRACT

Primary infection of a plant with a pathogen that causes high accumulation of salicylic acid in the plant typically via a hypersensitive response confers enhanced resistance against secondary infection with a broad spectrum of pathogens, including viruses. This phenomenon is called systemic acquired resistance (SAR), which is a plant-priming for adaption to repeated biotic stress. However, the molecular mechanisms of SAR-mediated enhanced inhibition, especially of virus infection, remain unclear. Here, we show that SAR against cucumber mosaic virus (CMV) in tobacco plants (*Nicotiana tabacum*) involves a calmodulin-like protein, rgs-CaM. We previously reported the antiviral function of rgs-CaM, which binds to and directs degradation of viral RNA silencing suppressors (RSSs), including CMV 2b, via autophagy. We found that rgs-CaM–mediated immunity is ineffective against CMV infection in normally growing tobacco plants but is activated as a result of SAR induction via salicylic acid signaling. We then analyzed the effect of overexpression of rgs-CaM on salicylic acid signaling. Overexpressed and ectopically expressed rgs-CaM induced defense reactions including cell death, generation of reactive oxygen species, and salicylic acid signaling. Further analysis using a combination of salicylic acid analogue BTH and Ca^{2+} ionophore, A23187, revealed that rgs-CaM functions as an immune receptor that induces salicylic acid signaling by simultaneously perceives both viral RSS and Ca^{2+} influx as infection cues, implying its autoactivation. Thus, secondary infection of SAR-induced tobacco plants with CMV seems to be effectively inhibited through 2b recognition and degradation by rgs-CaM, leading to reinforcement of antiviral RNA silencing and other salicylic acid–mediated antiviral responses.

IMPORTANCE

Even without an acquired immune system like that in vertebrates, plants show enhanced whole-plant resistance against secondary infection with pathogens; this so-called systemic acquired resistance (SAR) has been known for more than half a century and continues to be extensively studied. SAR-induced plants strongly and rapidly express a number of antibiotics and pathogenesis-related proteins targeted against secondary infection, which can account for enhanced resistance against bacterial and fungal pathogens but are not thought to control viral infection. This study showed that enhanced resistance against cucumber mosaic virus is caused by a tobacco calmodulin-like protein, rgs-CaM, which detects and counteracts the major viral virulence factor (RNA silencing suppressor) after SAR induction. rgs-CaM–mediated SAR illustrates the growth vs. defense trade-off in plants, as it targets the major virulence factor only under specific biotic stress conditions, thus avoiding the cost of constitutive activation while reducing the damage from virus infection.

INTRODUCTION

Being sessile, plants are exposed to pathogen attacks and diverse environmental stresses and are unable to evade exposure to subsequent attacks. Instead, plants retain the "memory" of experiences with pathogens and environmental stresses, enabling them to mount defense reactions to subsequent challenges more effectively. A number of antibiotics and pathogenesis-related proteins targeted against secondary infection are expressed more strongly and rapidly. This general phenomenon is called priming (1); priming induced by and against pathogens is called systemic acquired resistance (SAR) (2). SAR was discovered decades ago (3, 4) and has the potential to confer on crops

enhanced resistance against diverse pathogens; for this reason, induction of SAR using chemical and biological agents has been explored. Studies in recent decades have dramatically unveiled the molecular mechanisms of SAR (2). SAR-induced plants systemically accumulate salicylic acid (5), an important phytohormone for mediating immune responses to pathogens (6, 7), including viruses (8). In *Arabidopsis thaliana*, the primed state of SAR is partly attributed to the action of the genes encoding the non-expressor of pathogenesis-related proteins NPR1, NPR3, and NPR4, which have been shown to be salicylic acid receptors and mediators (9-12). In addition, epigenetic modifications in SAR-induced plants have been suggested to be involved in the primed state (13). The existence of transgenerational SAR (14) supports the involvement of epigenetic modifications because such modifications can be inherited in plants (15). Thus, the requirement of NPR1 for transgenerational SAR (14) implies that salicylic acid is also involved in the epigenetic modifications. Although systemic salicylic acid biosynthesis (i.e., including plant parts distant from the site of infection) is required for induction of SAR (6), salicylic acid derivatives and other chemical molecules recently have been identified as the systemic signaling molecules (5).

In contrast to our understanding of the mechanisms of how SAR is induced and maintained, even across generations, the exact mechanisms underlying the enhanced resistance against pathogens, especially viruses, at secondary infection sites in SAR-induced plants remain to be examined. One such mechanism may be RNA silencing, a major plant defense against diverse viruses, which is induced by double-stranded RNA (dsRNA) and targets its cognate RNAs for degradation (16, 17). RNA silencing and salicylic acid–mediated immunity cooperatively inhibit systemic infection by the plum pox virus (18). RNA-dependent RNA polymerase 1, which is involved in antiviral

94 immunity through its role in RNA silencing (19-23), is induced by salicylic acid (22,
95 23). The RNA silencing components dsRNA binding protein 4, Argonaute 2 (AGO2),
96 and AGO4 are involved in salicylic acid–mediated and nucleotide-binding site (NB)–
97 leucine-rich repeat (LRR)–mediated immunity (24-26). On the other hand, resistance
98 against cucumber mosaic virus (CMV) and tobacco mosaic virus was enhanced by
99 applying exogenous salicylic acid to an *A. thaliana* triple mutant of the Dicer-like genes
100 that was considered to completely lack antiviral RNA silencing, implying that SAR is
101 independent of RNA silencing (27).
102 In this study, we revealed that a tobacco calmodulin-like molecule (a regulator
103 of gene silencing calmodulin-like protein, thus designated rgs-CaM), is involved in
104 SAR against CMV. rgs-CaM was initially isolated in a screen of tobacco proteins that
105 interact with the helper component-proteinase (HC-Pro) of the tobacco etch virus (28).
106 HC-Pro is a multifunctional protein found in viruses that are members of the genus
107 *Potyvirus* and functions as an effector molecule that suppresses antiviral RNA silencing
108 (RNA silencing suppressor [RSS]) (29-31). In a previous study, rgs-CaM was shown to
109 be an endogenous RSS that suppresses virus-induced gene silencing (VIGS) by the
110 potato virus X (PVX) vector, which was developed from a member of the genus
111 *Potexvirus* (28). We and other groups confirmed that rgs-CaM has RSS activity (32-34)
112 and facilitates infection by viruses in the genus *Begomovirus* via its RSS activity (34,
113 35). However, we also observed an antiviral function of rgs-CaM: it binds to and directs
114 degradation of two viral RSSs, HC-Pro and CMV 2b, via autophagy, resulting in
115 reinforcement of antiviral RNA silencing in virus-infected cells (32). The present study
116 reconciled these antagonistic functions of rgs-CaM by revealing a phase change in the
117 rgs-CaM function: the antiviral function is dormant in normally growing plants and

activated after SAR is induced. Moreover, we found that rgs-CaM also functions as an immune receptor. Previously, necrotic symptoms and hypersensitive responses accompanied by programmed cell death were thought to be required for SAR induction (36). More recently, however, immune receptors, receptor-like kinases (RLK), and NB-LRR proteins, which mainly perceive pathogen invasion and mount defense responses in plants, have been shown to induce SAR via defense signaling regardless of whether cell death occurs (37, 38). In this study, we showed that rgs-CaM induces salicylic acid signaling via simultaneous perception of both viral RSS and calcium ion (Ca^{2+}) influx as virus infection cues, implying autoactivation of the antiviral function of rgs-CaM in SAR. This study shows that two conditional reactions of tobacco plants (*Nicotiana tabacum*) against CMV — recognition of CMV infection, which induces salicylic acid signaling, and inhibition of CMV infection after SAR induction — are mediated by a single host protein.

RESULTS

Overexpressed and ectopically expressed rgs-CaM induces cell death and defense reactions

We became aware of the association between rgs-CaM and other defense reactions other than RNA silencing, by observing transgenic tobacco plants that constitutively overexpressed the *rgs-CaM* gene under the control of the cauliflower mosaic virus (CaMV) 35S promoter. Among a dozen transgenic lines, two showed dwarfing, deformation, and partial necrosis on their leaves (Fig. 1Ai, B and C). These phenotypes were similar to those of lesion mimic mutants that involve hypersensitive response–like programmed cell death, which are accompanied by induction of reactive oxygen species

(ROS) and immune signaling components, including salicylic acid (39, 40). In the transgenic plants showing these phenotypes, cell death was observed (Fig. 1B), ROS were generated (Fig. 1C), and mRNA of the gene for pathogenesis-related protein 1a (*PR1a*), an indicator of activation of salicylic acid signaling (41), was induced in the leaves (Fig. 1Di, ii). The severity of the lesion mimic phenotype (Fig. 1Aii) and *PR1a* levels (Fig. 1Di, ii) varied both among and within rgs-CaM–overexpressing lines. These results with the previous our inoculation test that showed the enchnaced resistance against CMV in the Line rgs-CaM16 (32) indicate the possibility that the overexpressed rgs-CaM can induce cell death and immune responses and signaling, though it does not always do so. We confirmed this possibility by two additional experiments.

First, rgs-CaM was overexpressed in wild-type tobacco plants by infection with a PVX vector expressing rgs-CaM. Infection with this vector caused necrotic spots, whereas infection with the empty PVX vector or the vector expressing the rgs-CaM gene that lacks the initiation codon to express its encoded protein [PVX-rgs-CaM(-atg)] did not (Fig. 2A). *PR1a* was induced significantly in leaves inoculated with the PVX vector expressing rgs-CaM but not in leaves inoculated with either the empty PVX vector or PVX-rgs-CaM(-atg). Second, rgs-CaM was transiently expressed in protoplasts prepared from wild-type tobacco leaves. Protoplasts transfection with an expression cassette containing *rgs-CaM* under the control of the CaMV 35S promoter resulted in cell death and ROS generation (Fig. 2B and C). In contrast, protoplasts transfected with negative control expression cassette [rgs-CaM(-atg)] did not significantly increase cell death or ROS generation. Taken together, these data suggest that overexpressed and ectopically expressed rgs-CaM induces immune responses and salicylic acid signaling.

rgs-CaM is involved in salicylic acid signaling in response to CMV-Y infection

Because overexpressed and ectopically expressed rgs-CaM induced immune responses and salicylic acid signaling in transgenic plants (Figs 1 and 2), we assume that endogenous rgs-CaM is also involved in induction of these responses, including salicylic acid signaling. Viral infection induces various immune responses and signals that are mediated via phytohormones, including salicylic acid, and thus rgs-CaM may be involved in these responses. We tested this possibility using PVX and CMV.

When rgs-CaM–knockdown tobacco plants, in which rgs-CaM was suppressed by an inverted repeat (IR) transgene (32), were inoculated with PVX, the levels of PVX coat protein (CP) and genomic and subgenomic RNAs (*gPVX and sgPVX*) observed by western and northern blotting, respectively. *sgPVX* was similar to those in inoculated wild-type tobacco plants but CP and *gPVX* accumulated to a lesser extent (Fig. 3A). We re-examined whether rgs-CaM facilitates or inhibits PVX infection using real-time PCR with more individual plants for each genotype (n = 8). Two primer pairs to amplify cDNAs of PVX RNAs were used (Fig. 3B). One was designed to amplify the cDNA from PVX genomic RNA (RdRp) and another to amplify the cDNA from both genomic and subgenomic RNAs of PVX (CP). PVX RNAs accumulated slightly more in inoculated leaves of the rgs-CaM − knockdown plants, but a statistically significant difference was detected only for RdRp cDNA, indicative of PVX genomic RNA (Fig. 3B). In non-inoculated upper leaves, PVX RNAs appeared to accumulate more in the rgs-CaM–knockdown plants than in wild-type plants, but the difference was not statistically significant. We then examined whether salicylic acid signaling was induced

189 in these plants by examining the mRNA level of *PR1a*. The *PR1a* mRNA level
190 increased slightly but significantly in non-inoculated upper leaves of wild-type tobacco
191 plants (Fig. 3C). Similar results were obtained in the rgs-CaM–knockdown plants but
192 the differences with the wild-type plants were not significant. Our results suggest that,
193 even if rgs-CaM is involved in defense and induction of salicylic acid signaling against
194 PVX infection, its contribution is minimal. Reduced *rgs-CaM* mRNA levels were not
195 observed in mock-inoculated leaves of the rgs-CaM–knockdown plants in comparison
196 to those of wild-type plants though it reduced in rgs-CaM–knockdown plants in the
197 other cases (Fig. 3D). In a previous study, we obtained several lines of rgs-CaM–
198 knockdown plants (32) but could not propagate them because of their infertility. In the
199 rgs-CaM–knockdown tobacco plants used in the present study, we speculate that rgs-
200 CaM expression was not as severely suppressed and thus this line was fertile.
201 In contrast to the situation with PVX, we obtained quite different results with the
202 CMV Y strain (CMV-Y). CMV RNAs and CP accumulated to similar levels in both
203 wild-type and rgs-CaM knockdown tobacco plants (Fig. 4A). *PR1a* expression was
204 strongly induced in CMV-inoculated leaves of wild-type tobacco plants, but to a lesser
205 extent in the rgs-CaM–knockdown plants (Fig. 4B). Although there was no statistically
206 significant difference in *PR1a* levels in inoculated leaves between wild-type and rgs-
207 CaM–knockdown plants in the experiment shown in Fig. 4B, experiment 1 (n = 3), we
208 repeated the experiment with more samples (n = 9) and detected a significantly higher
209 *PR1a* level in the wild-type plants than in the knockdown plants (Fig. 4B, experiment
210 2). Moreover, reduced *PR1a* expression in CMV-Y-inoculated leaves of the rgs-CaM–
211 knockdown plants, compared with that in wild-type tobacco plants, was also detected
212 previously (32). However, *PR1a* mRNA levels in the upper leaves of plants infected

with CMV-Y (Fig. 4B) and in leaves inoculated with CMV that lacked the 2b RSS (CMVΔ2b) (Fig. 4D) were not lower in the rgs-CaM–knockdown plants than those in wild-type plants. This was even though CMV RNAs and CP accumulated similarly in both wild-type and rgs-CaM knockdown plants (Fig. 4C). Considering that rgs-CaM physically interacts with the dsRNA binding site of 2b (32) and is a calmodulin-like protein with EF-hand motifs that bind to Ca^{2+} and probably transduce the Ca^{2+} signal (42), these results led us to hypothesize that rgs-CaM is an immune receptor. According to our model, in CMV-Y-infected epidermal cells in an inoculated leaf, 2b is expressed by CMV-Y, Ca^{2+} influx is derived from wounding caused by mechanical inoculation with Carborundum (Fig. 5A), and salicylic acid signaling is reduced by knocking down of rgs-CaM (Fig. 4B, experiment 2). However, a non-inoculated upper leaf (Fig. 5B) and a leaf inoculated with CMVΔ2b (Fig. 5C) lack either 2b expression or Ca^{2+} influx, and salicylic acid signaling (*PR1a* expression) is not reduced by knocking down of rgs-CaM (Fig. 4B and D). Therefore, we hypothesize that rgs-CaM induces salicylic acid signaling through perception of both 2b and Ca^{2+} influx as cues of the initial infection with CMV-Y in inoculated leaves.

rgs-CaM induces salicylic acid signaling via perception of both Ca^{2+} and viral RSS

To examine this hypothesis, we used transgenic tobacco plants that constitutively express a viral RSS, i.e., either CMV 2b or HC-Pro of clover yellow vein virus (ClYVV); the latter was chosen because HC-Pro is known to interact with rgs-CaM (28, 32). We previously showed that the *PR1a* mRNA level did not increase in these transgenic tobacco plants, compared with that in wild-type tobacco plants though the *rgs-CaM* mRNA level somewhat increased in transgenic plants (32). *PR1a* expression

was monitored at different times in the transgenic tobacco plants after wounding stress caused by opening microperforations in leaves with a bundle of about 400 pins (Fig. 5D). *PR1a* expression was induced at a level detectable by RT-PCR in the transgenic plants expressing 2b and HC-Pro 24 h after wounding, but not in wild-type plants (Fig. 5E).

Wounding causes various changes and reactions associated with morphological damage in injured cells and surrounding cells, including Ca^{2+} influx and generation of ROS. In fact, ROS were generated at the wounding sites in leaves of both wild-type plants and transgenic tobacco plants expressing viral RSSs (Fig. 5D). To examine whether *PR1a* expression is caused by the Ca^{2+} influx that accompanies wounding, in addition to viral RSS, we infiltrated leaves of transgenic tobacco plants expressing 2b or HC-Pro with a Ca^{2+} ionophore, A23187, which causes external Ca^{2+} influx and thus elevates intracellular Ca^{2+} levels by increasing its ability to cross biological membranes.

At 24 h after infiltration with A23187, *PR1a* was induced in transgenic tobacco plants expressing 2b or HC-Pro but not in transgenic tobacco plants expressing CMV CP or in wild-type tobacco plants (Fig. 6A). We confirmed that the *PR1a* expression was not due to a side effect of A23187: infiltration of A23187 did not cause cell death or other obvious morphological changes in these plant leaves (Fig. 6B), and concurrent treatment with ethylene glycol-bis(β-aminoethyl ether)-*N*,*N*,*N'*,*N'*-tetraacetic acid (EGTA), which chelates Ca^{2+}, and A23187 antagonized *PR1a* expression (Fig. 6Ci). We note that *PR1a* was slightly induced in wild-type plants with A23187 infiltration (Fig. 6Cii). However, this slight *PR1a* induction seems to be qualitatively different from that induced by viral RSSs and Ca^{2+} influx, because the *PR1a* mRNA levels that were increased by Ca^{2+} in 2b-expressing plants were reduced in the presence of EGTA,

whereas the *PR1a* levels induced by Ca^{2+} in wild-type plants treated with A23187 did not change in the presence of EGTA. We conclude that the expression of an RSS together with Ca^{2+} influx induces salicylic acid signaling but that neither RSS expression nor Ca^{2+} influx alone is sufficient. Ca^{2+} influx induced rgs-CaM expression (Fig. 6Ci, ii), consistent with our hypothesis that *PR1a* is induced via rgs-CaM. To test this further, we used a PVX vector that expresses the *rgs-CaM* mRNA sequence without its initiation codon to knock down the expression of endogenous rgs-CaM by VIGS [VIGS(rgs-CaM)]. When RSS-expressing tobacco plants were inoculated with the PVX empty vector, *PR1a* expression was induced even without A23187 treatment (Fig. 7A). We also found induction of *PR1a* in the empty-vector-infected wild-type tobacco plants treated with A23187. *PR1a* induction by infection of RSS-expressed plants with PVX without A23187 or by infiltration of PVX-infected tobacco leaves with A23187 is apparently discrepant to our hypothesis shown in Fig. 5A and discussed later in the Discussion section. Including these apparently discrepant cases, the *PR1a* inductions were reduced by infection with the VIGS(rgs-CaM) vector (Fig. 7A), suggesting that *PR1a* induction depends on rgs-CaM.

PR1a induction was suppressed when salicylate hydroxylase (*NahG*)-expressing tobacco plants, in which salicylic acid is converted to catechol and thus salicylic acid signaling is antagonized, were inoculated with the PVX empty vector or CMVΔ2b and then treated with A23187. These results indicate that salicylic acid signaling was induced in wild-type tobacco plants infected with either the empty PVX vector or CMVΔ2b infection when Ca^{2+} influx was artificially induced with A23187 (Fig. 7B).

rgs-CaM is necessary for enhanced resistance against CMV in SAR-induced

tobacco plants

In addition to being an inducer of salicylic acid signaling, we found that rgs-CaM is involved in salicylic acid–mediated antiviral defense. The inoculation test results in Fig. 4 showed comparable accumulation of CMV CP and genomic RNAs in inoculated and upper leaves between wild-type and rgs-CaM–knockdown plants, indicating that rgs-CaM does not interfere with CMV infection. However, when CMV was inoculated into relatively old tobacco plants (for example, 7 weeks after sowing [Fig. 8Ai]), the rgs-CaM–knockdown plants developed systemic yellowing of leaves earlier than did the inoculated wild-type plants. At 16 dpi, CMV could be detected by western blotting only in non-inoculated upper leaves of inoculated rgs-CaM–knockdown plants (Fig. 8Aii). The tobacco plants described in Fig. 4 were inoculated at 4 weeks after sowing, suggesting that the antiviral function of rgs-CaM has two phases: it is dormant in normally growing young tobacco plants around 4 weeks after sowing but becomes activated by 7 weeks after sowing.

What, then, is different between tobacco plants at 4 and 7 weeks after sowing that brings about the phase change of the antiviral function of rgs-CaM? A previous study showed that tobacco plants gradually accumulate salicylic acid during the 7 to 10 weeks after sowing and develop enhanced resistance against tobacco mosaic virus, probably because of the accumulated salicylic acid (43). Similar age- and salicylic acid-related resistance against CMV has been reported previously (44, 45). These studies prompted us to examine whether salicylic acid signaling affects rgs-CaM function by using a salicylic acid analog, benzo-(1,2,3)-thiadiazole-7-carbothioic acid S-methyl ester (BTH), which is a strong inducer of SAR via systemic induction of salicylic acid signaling (46, 47). Systemic symptom expression in leaves was delayed (Fig. 8Bi) and

CMV accumulation was drastically reduced in BTH-treated wild-type tobacco plants relative to the untreated control (Fig. 8Bii, iii), confirming the enhancement of antiviral resistance by induction of SAR with BTH, as reported previously (48, 49). These effects were weakened in the rgs-CaM–knockdown plants, indicating that the enhanced resistance to CMV induced by BTH depends on rgs-CaM (Fig. 8Bii, iii). Judging by the symptoms observed (Fig. 8Bi) and the results of western blotting with samples of inoculated leaves (Fig. 8Bii), some resistance was still induced in BTH-treated rgs-CaM–knockdown plants. This resistance might have been caused by the residual rgs-CaM in the knockdown plants or by a salicylic acid–mediated defense system that operates independently but in parallel to the rgs-CaM-mediated defense mechanism. To examine whether tobacco plants have salicylic acid-mediated defense system(s), which is not linked to the rgs-CaM-mediated defense mechanism, we conducted similar experiments using CMVΔ2b and PVX because these viruses were considered to lack an RSS that interact with rgs-CaM. When CMVΔ2b was inoculated into wild-type tobacco plants, CMVΔ2b accumulation was drastically reduced by BTH-treatment even in rgs-CaM–knockdown plants (Fig. 8C), indicating the existence of independent salicylic acid-mediated defense system(s) that effectively inhibit CMV infection. When PVX was inoculated into wild-type tobacco plants in which SAR was induced by pretreatment with BTH, PVX CP accumulated in inoculated and upper leaves, although to a slightly lesser extent than in non-induced leaves (Fig. 8D). Similar results were obtained using the rgs-CaM–knockdown tobacco plants. Thus, the SAR induced by BTH was relatively ineffective against PVX, compared with that against CMV-Y and CMVΔ2b, and we could not conclude whether rgs-CaM contributes to the low level of SAR against PVX.

Reduced accumulation of viral RSSs in SAR-induced transgenic tobacco cells and plants

We previously demonstrated that rgs-CaM binds to and directs degradation of viral RSSs, CMV 2b and ClYVV HC-Pro, via autophagy (32). The prerequisite of rgs-CaM for enhanced resistance against CMV but not against CMVΔ2b in SAR-induced plants implies that the rgs-CaM–mediated degradation of viral RSSs might be activated in the SAR-induced plants. Using cultured transgenic tobacco BY2 cells that constitutively express CMV 2b, we examined whether the degradation of 2b is activated by SAR induction. The 2b protein was detected in nuclei in untreated cells by immunofluorescent staining, but the fluorescent signal disappeared 1 h after BTH treatment (Fig. 9). The fluorescent signal was, however, retained in cells treated with both BTH and an autophagy inhibitor (either E64d or concanamycin A), suggesting that the degradation of 2b, probably via autophagy, was activated by SAR induction, which leads to resistance against CMV-Y infection.

We then examined the effect of Ca^{2+} influx on accumulation of the HC-Pro protein in SAR-induced HC-Pro transgenic tobacco plants because Ca^{2+} influx is expected as a result of wounding during virus infection, as illustrated in Fig. 5A–C. A23187 treatment reduced accumulation of the HC-Pro protein in SAR-induced HC-Pro tobacco plants (Fig. 10A). However, A23187 treatment had little effect on accumulation of the HC-Pro protein in HC-Pro tobacco plants in which SAR was not induced, suggesting that HC-Pro expression is specifically inhibited in the initial virus-infected cells of SAR-induced tobacco plants. The upper band (around 25 kDa) of the rgs-CaM protein extracted from A23187-infiltrated leaf tissue of SAR-induced plants migrated a

357 little more slowly in SDS-PAGE than that extracted from A23187-infiltrated leaf tissue
358 of non-induced plants (Fig. 10A, right panel, blue arrowheads), implying a change in
359 the rgs-CaM protein state as a result of SAR induction.
360
361 **DISCUSSION**
362 This study revealed that a novel class of protein, calmodulin-like protein rgs-CaM,
363 functions as an immune receptor for CMV infection and induces salicylic acid
364 signaling, which is characteristic of immune responses against biotrophic pathogens,
365 including viruses (8), and is required for SAR induction (2, 6). As mentioned in the
366 Introduction, the known immune receptors for pathogens in plants are mostly RLKs and
367 NB-LRRs. RLKs perceive molecules that are conserved among pathogenic
368 microorganisms but are not found in host plants (pathogen- or microorganism-
369 associated molecular patterns [PAMPs or MAMPs]) and induce pattern-triggered
370 immunity (PTI). Host-adapted pathogens develop effector molecules that suppress PTI
371 and enable their colonization of plants. Another class of receptors, NB-LRRs,
372 counteractively recognize pathogen effector proteins and induce strong defense
373 reactions, called hypersensitive responses; this mechanism is termed effector-triggered
374 immunity (ETI) (50, 51). Several NB-LRRs that perceive virus invasion and induce ETI
375 have been identified (52), and recent studies of *Arabidopsis* RLKs (53, 54) suggests the
376 existence of an immune receptor that perceives dsRNAs or other viral factors as viral
377 PAMPs and induces PTI. In animals, Toll-interleukin 1-like receptors (TLRs), which are
378 structurally similar to plant RLKs and NB-LRRs, perceive viral RNA and DNA in
379 endosomes and on cell membranes (55). In addition, RIG-I and MDA5 for viral RNA
380 and IFI16 and cGAS for viral DNA have been identified as receptors that perceive

PAMPs in the cytoplasm and nucleus (56). A NOD-like receptor and other host factors have been implicated in recognition of viral infection (56). However, no CaM or CaM-like protein (CML) has previously been identified to be an immune receptor.

Plant CaMs and CMLs are Ca^{2+} sensors that play important roles in development and stress responses (57, 58). An increase in the Ca^{2+} concentration in the cytoplasm is one of the earliest events following exposure to environmental stresses and Ca^{2+} is a crucial secondary messenger in the perception of these stresses. In plants, CaMs and CMLs constitute a relatively large family of Ca^{2+} sensor genes along with two other classes of proteins, calcineurin B-like proteins and Ca^{2+}-dependent protein kinases (59). CaMs and CMLs bind a number of endogenous factors and have no obvious functional domains except for 1−7 EF-hand motifs for binding Ca^{2+}, and thus are considered to transduce Ca^{2+} signals by modifying the activity or conformation of their binding endogenous proteins (58). rgs-CaM, one of the tobacco CMLs, uniquely binds to exogenous proteins, diverse viral RSSs [including potyvirus HC-Pro, CMV, (the related) tomato aspermy virus 2b and human immunodeficiency virus TAT], presumably via affinity to their positively charged dsRNA-binding sites (28, 32), though there is no conserved amino acid sequence motif among these dsRNA-binding domains. CaMs and CMLs are hub proteins, which bind to various substrate proteins through their relatively disordered binding sites (60). Homology modeling (32, 42) implies that rgs-CaM has a negatively charged disordered binding site for substrates, which is probably where rgs-CaM binds diverse viral RSSs. Since viral RSSs are considered to be effectors that suppress an antiviral PTI-like basal defense (RNA silencing), rgs-CaM is another class of receptor for viral effectors in addition to NB-LRRs. rgs-CaM perceives not only viral RSSs but also Ca^{2+} cues that induce salicylic acid signaling (Figs. 4 to 7). A recent

405 structural and thermodynamic study by Makiyama et al. (42) revealed that rgs-CaM
406 binds Ca^{2+} at three EF-hand motifs and suggested that Ca^{2+} binding at the two EF hands
407 that show higher affinity to Ca^{2+} alters the conformation of rgs-CaM such that the
408 negatively charged binding sites are more exposed. This supports our model that
409 salicylic acid signaling is induced by the dual perception of viral RSS and Ca^{2+} by rgs-
410 CaM (Figs. 5A to C and 10B). We assume that the dual perception of viral RSS and
411 Ca^{2+} by rgs-CaM avoids nonspecific induction of salicylic acid signaling. Consistently,
412 overexpression and ectopic expression of rgs-CaM did not always induce defense
413 responses and salicylic acid signaling (Fig. 1). Because plant cells are surrounded by a
414 cell wall, virus invasion seems to require mechanical wounding, which would cause
415 Ca^{2+} influx in the virus-invaded cells. The normal mechanism of CMV infection in the
416 field is via aphid feeding and aphid feeding has been reported to cause Ca^{2+} influx in
417 tobacco plants (61, 62). In general, defense responses against various abiotic and biotic
418 stress responses involve Ca^{2+} fluxes (63), and virus infection is known to lead to an
419 increase of the cytoplasmic Ca^{2+} concentration (64). We assume this is why *PR1a* was
420 induced in PVX-infected transgenic tobacco plants expressing viral RSSs without
421 artificial Ca^{2+} influx induced by A23187 (Fig. 7A). Therefore, the dual perception of a
422 viral component and Ca^{2+} seems suitable as a viral infection cue to specifically induce
423 immune responses. One drawback to recognition of a viral RSS as an infection cue is
424 that it is incapable of immediate induction of immune responses because most viral
425 RSSs, including 2b and HC-Pro, are not included in the invading virion, but are
426 expressed during establishment of viral infection and viral multiplication. As described
427 below, the rgs-CaM-induced immune responses do not appear to prevent primary virus
428 infection; rather, salicylic acid signaling among them may contribute to prevent

429 subsequent infection by viruses possessing RSSs that interact with rgs-CaM via its
430 autoactivation in SAR-induced plants. Therefore, the rgs-CaM–induced immune
431 responses do not necessarily need to be induced immediately. In the present study, the
432 induction of rgs-CaM–mediated salicylic acid signaling after wounding of transgenic
433 plants expressing viral RSSs took 24 h (Fig. 5E), which is slower than that seen with
434 ETI (hypersensitive response) (65).

435 rgs-CaM may have the ability to induce salicylic acid signaling in response to
436 viral or host proteins other than viral RSS. Under natural conditions, rgs-CaM does not
437 seem to be involved in induction of salicylic acid signaling in response to PVX and
438 CMVΔ2b infection (Figs. 3 and 4). However, when Ca^{2+} influx was artificially induced
439 with A23187 in wild-type plants, salicylic acid signaling was induced by infection with
440 either PVX or CMVΔ2b (Fig. 7), and salicylic acid signaling induced by PVX in the
441 presence of Ca^{2+} was dependent on rgs-CaM (Fig. 7A). The triple gene block protein1
442 (TGBp1) of PVX is an RSS. The suppression mechanism of RNA silencing by TGBp1
443 is not through binding to dsRNA; instead, TGBp1 was reported to bind to AGO1–
444 AGO4 and lead to degradation of AGO1 via the 26S proteasome (66). Considering that
445 rgs-CaM probably binds to the dsRNA binding sites of viral RSSs, rgs-CaM may not
446 bind TGBp1. More strikingly, tobacco plants must be able to recognize CMV proteins
447 other than its RSS (2b) for there to be induction of salicylic acid signaling by CMVΔ2b
448 (Fig. 7B). At first glance, the results in Fig. 7 seem to contradict our conclusion that rgs-
449 CaM perceives viral RSSs and Ca^{2+} as virus infection cues to induce salicylic acid
450 signaling. One possible explanation is that rgs-CaM may have weak affinity to PVX and
451 CMV protein(s) other than 2b, and can bind to them when Ca^{2+} influx is stimulated by
452 A23187 infiltration (Fig. 10B, right panel). The substrate (RSS) binding domain of rgs-

453 CaM was predicted to be more exposed when Ca^{2+} binds to rgs-CaM at its EF hands
454 (42). Therefore, under specific conditions, such as when wild-type tobacco leaves that
455 were infected with PVX or CMV Δ2b were subsequently infiltrated with A23187, rgs-
456 CaM may perceive other PVX and CMV protein(s) to induce salicylic acid signaling.
457 Another possibility is simply that rgs-CaM binds to host intermediate(s) that is induced
458 by virus infection for salicylic acid signaling.
459 RNA silencing and salicylic acid–mediated immunity are two major antiviral
460 systems in plants and their linkage has been suggested (18-26). The present study also
461 revealed a link between RNA silencing and salicylic acid–mediated immunity via a
462 single host factor, rgs-CaM, which suppresses antiviral RNA silencing as an
463 endogenous RSS but induces salicylic acid signaling by perceiving viral RSS as an
464 immune receptor (e.g., in the case of CMV). Pruss et al. (67) reported that transgenic
465 tobacco plants expressing HC-Pro show enhanced resistance to both heterologous
466 viruses that have different RSSs and fungal pathogens; depending on the pathogen,
467 resistance could be either salicylic acid–dependent or –independent. The mechanism
468 underlying this viral RSS–induced enhanced resistance against multiple pathogens
469 remains unclear. In those transgenic plants (68), rgs-CaM could induce salicylic acid
470 signaling in response to Ca^{2+} influx caused by infection with pathogens and thus partly
471 contribute to the enhanced resistance in a salicylic acid–dependent manner.
472 Another significant observation of this study is uncovering a part of the
473 molecular mechanism underlying the enhanced resistance against a virus in SAR-
474 induced plants. We previously reported the antiviral function of rgs-CaM (32). The
475 present study revealed that this antiviral function is not constitutively active but exhibits

476 a phase change from dormant to activated after SAR induction via salicylic acid
477 signaling (Figs. 4, 8–10). We previously showed that, without artificial induction of
478 SAR, the rgs-CaM–overexpressing transgenic tobacco plants (rgs-CaM16) inhibit CMV
479 infection (32). However, this is not contradictory to the present study because
480 overexpression of rgs-CaM induces salicylic acid signaling systemically in this
481 transgenic line (Fig. 1) and thus induces SAR. Since CMV infection has been reported
482 to induce salicylic acid signaling in this study (Fig. 4) and previously (44, 68, 69), one
483 may expect that rgs-CaM autoactivates its antiviral function for SAR during CMV
484 infection via its perception of CMV 2b. However, rgs-CaM did not effectively inhibit
485 CMV infection in relatively young plants (Fig. 4) though it did in older plants (Fig. 8A).
486 CMV 2b has been reported to interfere with salicylic acid and jasmonic acid signaling
487 (44, 68, 69). Ca^{2+} influx induced by A23187 caused rgs-CaM protein accumulation in
488 both wild-type and 2b-expressing transgenic plants (Fig. 6C). However, its
489 accumulation level was lower in 2b-expressing plants, in which *PR1a* was induced, than
490 in wild-type tobacco plants. Our previous study (32) suggested that both rgs-CaM and
491 viral RSS proteins are posttranslationally regulated via the 26S proteasome and
492 autophagy and that rgs-CaM directs degradation of these RSS proteins. The rgs-CaM–
493 mediated degradation of viral RSS proteins, was enhanced by salicylic acid signaling
494 (Figs. 8 − 10). Overexpression of *rgs-CaM* did not always result in increased
495 accumulation of rgs-CaM protein, induction of salicylic acid signaling, and other
496 defense responses (Fig. 1), suggesting complex interactions (counteraction or
497 neutralization) among rgs-CaM, 2b, salicylic acid signaling and protein degradation
498 pathways.

It is generally assumed that plants and animals inhibit infection by any pathogens to reduce the threat of disease. However, this and previous studies have shown biased reactions of tobacco plants against pathogenic viruses via the antagonistic functions of rgs-CaM. rgs-CaM was initially shown to be an endogenous RSS by using transgenic *N. benthamiana* in which the tobacco *rgs-CaM* gene was overexpressed by the CaMV 35S promoter (28). In that study, the overexpressed tobacco *rgs-CaM* interfered with VIGS of GFP by a PVX vector, resulting in increased fluorescence and accumulation of the GFP transgene and the PVX genomic RNA itself (28). Li et al. (34) reported that infection by tomato yellow leaf curl China virus, a member of the genus *Begomovirus*, was facilitated or inhibited in transgenic *N. benthamiana* plants in which rgs-CaM was overexpressed or silenced, respectively. They also confirmed the RSS activity of rgs-CaM (34, 70). Additionally, infection by tomato golden mosaic virus, another member of the genus *Begomovirus*, was shown to be facilitated in transgenic *Arabidopsis* plants in which *Arabidopsis* CML39, one of the proteins most similar to rgs-CaM among 50 *Arabidopsis* CMLs, was overexpressed (35). Taken together with data in this study, in normally growing plants, rgs-CaM facilitates infection by members of the genus *Begomovirus*, but not CMV (*Cucumovirus*) and PVX (*Potexvirus*), probably by its RSS activity, but inhibits CMV infection by its phase-changed antiviral activity that directs degradation of CMV 2b via autophagy after SAR induction.

Constitutive activation of plant immune systems results in inhibition of plant growth (71), as also shown here by overexpression of rgs-CaM (Fig. 1). This trade-off between immunity and growth in plants has driven the evolution of immune receptors for recognition of pathogen invasion that effectively induce defense mechanisms only when needed. The receptor and conditional effector functions of rgs-CaM (that is, its

phase change via SAR induction) suggest that tobacco changes its reaction to viral infection according to environmental conditions via rgs-CaM. rgs-CaM strongly inhibits infection by viruses that express RSSs that directly interact with it, such as CMV, only under environmental conditions with a high frequency of infection by pathogens, which leads to SAR induction (Fig. 10B, left and center panels). In general, viral RSSs function as virulence factors not only by enhancing virus multiplication that leads to increased expression of other viral virulence factors via suppressing antiviral RNA silencing, but also by disrupting host gene expression controlled by the small-RNA pathways in infected cells. This biased and conditional antiviral defense system has presumably developed as a means of counteracting RSS-expressing virulent viruses to avoid the cost of constitutive defense activation while reducing the damage from the virus infection.

MATERIALS AND METHODS

PVX vectors carrying rgs-CaM cDNA and expression cassettes

The *rgs-CaM* ORF and the ORF lacking its initial codon were cloned between the *Cla*I and *Sal*I sites of the PVX vector pPC2S (72) to generate PVX-rgs-CaM and PVX-rgs-CaM(-atg) [VIGS(rgs-CaM)], respectively. After linearization of these plasmids by digestion with *Spe*I, infectious RNAs were transcribed by T7 RNA polymerase with the 7-methylguanosine-5′-phosphate cap analog (Thermo Fisher Scientific Inc., Waltham, MA, USA) from the linearized plasmids and used as inocula for mechanical inoculation. The *rgs-CaM* ORFs with/without the initiation codon were also cloned between the *Xba*I and *Sac*I sites of pE2113 (73) and the cloned plasmids, pE2113-rgs-CaM and

pE2113-rgs-CaM(-atg), were used for transfection of tobacco protoplasts to express rgs-CaM under control of the CaMV 35S promoter.

Transgenic tobacco plants and virus inoculation

Transgenic tobacco plants (*N. tabacum* cv. Xanthi), in which rgs-CaM was either overexpressed or knocked down, were made previously (32). Transgenic tobacco plants (*N. tabacum* cv. BY4) expressing viral RSSs were also made previously (32). Transgenic tobacco plants expressing CMV CP and NahG were made similarly to those expressing viral RSSs (32). T2 or later generations of transgenic tobacco plants, all of which were shown to be kanamycin resistant, were grown under a 16-h light/8-h dark photoperiod at 25°C for virus inoculation and other experiments. *N. benthamiana* leaves infected with CMV-Y; CMVΔ2b, which lacked 2b and was designated CMV-H1 in a previous study (74); and the PVX vectors were used as inocula for mechanical inoculation with Carborundum and stored in a deep freezer at −80°C until needed.

BTH and Ca^{2+} ionophore treatment

A salicylic acid analog, BTH, was spread on tobacco leaves with cotton tufts that were dipped in 1 mM BTH, 1.4% (vol/vol) acetone as a solvent, and 0.2% Tween-20. Phosphate-buffered saline (PBS; 137 mM NaCl, 2.7 mM KCl, 10 mM $Na_2HPO_4 \cdot 12H_2O$, and 2 mM KH_2PO_4 pH 7.4) containing 75 μM of Ca^{2+} ionophore A23187 (MilliporeSigma, St. Louis, MO, USA) was prepared by diluting A23187 stock solution (5 mg/ml of A23187 dissolved in DMSO) with PBS, and the diluted A23187 solution with/without 10 mM EGTA was infiltrated into leaves with a syringe.

Preparation, transfection, and assays of tobacco protoplasts

Tobacco mesophyll protoplasts were prepared from wild-type tobacco plants (*N. tabacum* cv. Xanthi) and transfected with pE2113 vectors as described previously (75). Assays following transfection were also carried out according to the method from the previous study (75). H_2O_2 signals, indicative of ROS generation, were visualized with 500 nM 2′,7′-dichlorofluorescein-diacetate (H_2DCF) (MilliporeSigma) 5 h after transfection. The images were observed with a fluorescence microscope (Leica DMI 6000B; Leica, Tokyo) and H_2DCF signals were visualized with excitation at 488 nm (emission: 498 to 532 nm). Eleven hours after transfection, protoplasts were exposed to 0.04% Evans blue dye (an indicator of cell death) for 5 min and then observed with light microscopy (Olympus BX51; Olympus, Tokyo).

RT-PCR, semi-quantitative RT-PCR, real-time RT-PCR, and northern blotting

After tobacco leaves were ground in liquid nitrogen, total RNA was extracted using the TRIzol reagent according to the manufacturer's manual (Thermo Fisher Scientific). Each RNA sample was treated with RNase-free DNase I (Roche Diagnostics, Basel, Switzerland). First-strand cDNAs were synthesized from 1 μg of RNA extracts by a modified M-MLV reverse transcriptase, ReverTra Ace (Toyobo, Osaka, Japan). Accumulation of viral genomic RNAs and endogenous mRNAs was detected by PCR in a mixture (25 μl) containing cDNAs corresponding to 0.05 μg RNA, 0.4 μM of each of the specific primer pairs listed in Table 1, 0.2 mM dNTP, and 0.625 U Ex Taq DNA polymerase (TaKaRa, Otsu, Japan). PCR mixtures for *PR1a* were incubated for 2 min at 94°C, followed by 28 cycles of 94°C for 30 s, 62°C for 30 s, and 72°C for 40 s, and PCR products were fractionated with 2% agarose gel electrophoresis. Semi-quantitative

RT-PCR was done for rgs-CaM by using 24 cycles of 94°C for 30 s, 59°C for 30 s, and 72°C for 30 s, and for 18S rRNA by using 15 cycles of 94°C for 30 s, 58°C for 30 s, and 72°C for 30 s. Real-time PCR was performed by using the DNA Engine Opticon 2 system (Bio-Rad Laboratories, Hercules, CA, USA) according to the method in a previous study (76). The reaction mixture (25 μl) contained 0.625 U of Ex Taq (TaKaRa), Ex Taq buffer, 0.2 mM dNTP, 0.2 μM (each) forward and reverse primers listed in Table 1, SYBR Green (30,000 × dilution) (Thermo Fisher Scientific), and cDNA corresponding to 12.5 ng of total RNA. Samples were incubated for 2 min at 95°C, followed by 39 cycles of 95°C for 10 s, 58°C for *rgs-CaM* or 59°C for *PR1a* for 20 s, and 72°C for 20 s. Northern blotting was performed as described previously (77) using DIG-labeled cRNA probes (Roche Diagnostics). These probes were made from the target mRNA sequences, PVX genomic RNA sequence, and the conserved nucleotide sequence at the 3′-terminal regions of CMV genome segments using the primers listed in Table 1. RNA samples (2–5 μg) were fractionated by denaturing agarose gel electrophoresis and transferred onto a nylon membrane (Hybond-N; GE Healthcare, Chicago, IL, USA). Chemiluminescence signals were quantitatively detected by a LAS-4000 mini PR Lumino-image analyzer (GE Healthcare).

Western blotting

Western blotting was carried out as described previously (32). Tobacco leaf tissues were homogenized in liquid nitrogen and then dissolved in 12-fold (volume/mass) urea-denaturing buffer containing 4.5 M urea, 1% (vol/vol) Triton X-100, 0.5% DTT, 0.0625 M Tris-HCl pH 6.8, 2% (wt/vol) SDS, 5% mercaptoethanol, 5% sucrose, and 0.002%

bromophenol blue. The extracts were centrifuged to collect the supernatants. Equal amounts of samples were separated by 10% SDS/PAGE. Fractionated proteins were then transferred to Immobilon PVDF membranes (MilliporeSigma), and the blots were probed with anti-PVX CP, anti-CMV CP, anti-2b, and anti-rgs-CaM rabbit polyclonal antibodies. Proteins were visualized using antirabbit secondary antibodies conjugated to alkaline phosphatase, followed by treatment with CDP-Star solutions (Roche Diagnostics, Basel, Switzerland) for chemiluminescence detection. Chemiluminescent signals were quantitatively detected by a LAS-4000 mini PR Lumino-image analyzer (GE Healthcare).

Immunohistochemical studies with tobacco BY2 cultured cells

Tobacco BY2 cultured cells were transformed with the CMV 2b gene under the control of the CaMV 35S promoter in a previous study (78), in which the transformed BY2 was called cell line Y2b–BY2. Transgenic BY2 cells expressing 2b were pretreated with 10 μM BTH with/without autophagy inhibitors E64d (10 μM) and concanamycin A (0.1 μM) for 1 h and then assayed for endogenous rgs-CaM and CMV 2b as described previously (32). The fixed cells were immunofluorescently stained with their specific primary and CF594 goat antirabbit IgG secondary antibodies (Biotium, Fremont, CA, USA). These cells were also fluorescently stained with 4′,6-diamino-2-phenylindole (DAPI) to detect nuclei. Photomicrographs were taken using a Leica DMI6000 B microscope (Leica Microsystems). Image colors were then reassigned using AF6000 ver. 1.5 software.

ACKNOWLEDGEMENTS

We thank Dr. Peter Palukaitis for critical reading of this manuscript. This work was supported in part by Japan Society for the Promotion of Science (JSPS) KAKENHI grant numbers 25450055 and 16H04879 to K.S.N., the NOVARTIS Foundation (to K.S.N.), and the Asahi Glass Foundation (to K.S.N.). The authors declare no competing financial interests.

REFERENCES

1. **Savvides A, Ali S, Tester M, Fotopoulos V.** 2016. Chemical priming of plants against multiple abiotic stresses: mission possible? Trends Plant Sci **21:**329–340.

2. **Fu ZQ, Dong X.** 2013. Systemic acquired resistance: turning local infection into global defense. Annu Rev Plant Biol **64:**839–863.

3. **Gilpatrick JD, Weintraub M.** 1952. An unusual type of protection with the carnation mosaic virus. Science **115:**701–702.

4. **Chester KS.** 1933. the problem of acquired physiological immunity in plants. Q Rev Biol **8:**129–154, 275–324.

5. **Gao QM, Zhu S, Kachroo P, Kachroo A.** 2015. Signal regulators of systemic acquired resistance. Front Plant Sci **6:**228.

6. **Delaney TP, Uknes S, Vernooij B, Friedrich L, Weymann K, Negrotto D, Gaffney T, Gut-Rella M, Kessmann H, Ward E, Ryals J.** 1994. A central role of salicylic acid in plant disease resistance. Science **266:**1247–1250.

7. **Wildermuth MC, Dewdney J, Wu G, Ausubel FM.** 2001. Isochorismate synthase is required to synthesize salicylic acid for plant defence. Nature **414:**562–565.

8. **Palukaitis P, Carr JP.** 2008. Plant resistance responses to viruses. J Plant Pathol **90:**153–171.

9. **Cao H, Glazebrook J, Clarke JD, Volko S, Dong X.** 1997. The Arabidopsis *NPR1* gene that controls systemic acquired resistance encodes a novel protein containing ankyrin repeats. Cell **88:**57–63.

10. **Fu ZQ, Yan S, Saleh A, Wang W, Ruble J, Oka N, Mohan R, Spoel SH,**

Tada Y, Zheng N, Dong X. 2012. NPR3 and NPR4 are receptors for the immune signal salicylic acid in plants. Nature **486:**228–232.

11. **Attaran E, He SY.** 2012. The long-sought-after salicylic acid receptors. Mol Plant **5:**971–973.

12. **Wu Y, Zhang D, Chu JY, Boyle P, Wang Y, Brindle ID, De Luca V, Despres C.** 2012. The *Arabidopsis* NPR1 protein is a receptor for the plant defense hormone salicylic acid. Cell Rep **1:**639–647.

13. **Conrath U, Beckers GJ, Langenbach CJ, Jaskiewicz MR.** 2015. Priming for enhanced defense. Annu Rev Phytopathol **53:**97–119.

14. **Luna E, Bruce TJ, Roberts MR, Flors V, Ton J.** 2012. Next-generation systemic acquired resistance. Plant Physiol **158:**844–853.

15. **Hauser MT, Aufsatz W, Jonak C, Luschnig C.** 2011. Transgenerational epigenetic inheritance in plants. Biochim Biophys Acta **1809:**459–468.

16. **Pumplin N, Voinnet O.** 2013. RNA silencing suppression by plant pathogens: defence, counter-defence and counter-counter-defence. Nat Rev Microbiol **11:**745–760.

17. **Incarbone M, Dunoyer P.** 2013. RNA silencing and its suppression: novel insights from in planta analyses. Trends Plant Sci **18:**382–392.

18. **Alamillo JM, Saenz P, Garcia JA.** 2006. Salicylic acid-mediated and RNA-silencing defense mechanisms cooperate in the restriction of systemic spread of plum pox virus in tobacco. Plant J **48:**217–227.

19. **Cao M, Du P, Wang X, Yu YQ, Qiu YH, Li W, Gal-On A, Zhou C, Li Y, Ding SW.** 2014. Virus infection triggers widespread silencing of host genes by a distinct class of endogenous siRNAs in *Arabidopsis*. Proc Natl Acad Sci USA **111:**14613–14618.

20. **Garcia-Ruiz H, Takeda A, Chapman EJ, Sullivan CM, Fahlgren N, Brempelis KJ, Carrington JC.** 2010. *Arabidopsis* RNA-dependent RNA polymerases and dicer-like proteins in antiviral defense and small interfering RNA biogenesis during *Turnip mosaic virus* infection. Plant Cell **22:**481–496.

21. **Yang SJ, Carter SA, Cole AB, Cheng NH, Nelson RS.** 2004. A natural variant of a host RNA-dependent RNA polymerase is associated with increased susceptibility to viruses by *Nicotiana benthamiana*. Proc Natl Acad Sci USA **101:**6297–6302.

22. **Yu D, Fan B, MacFarlane SA, Chen Z.** 2003. Analysis of the

involvement of an inducible *Arabidopsis* RNA-dependent RNA polymerase in antiviral defense. Mol Plant-Microbe Interact **16:**206–216.

23. **Xie Z, Fan B, Chen C, Chen Z.** 2001. An important role of an inducible RNA-dependent RNA polymerase in plant antiviral defense. Proc Natl Acad Sci USA **98:**6516–6521.

24. **Zhu S, Jeong RD, Lim GH, Yu K, Wang C, Chandra-Shekara AC, Navarre D, Klessig DF, Kachroo A, Kachroo P.** 2013. Double-stranded RNA-binding protein 4 is required for resistance signaling against viral and bacterial pathogens. Cell Rep **4:**1168–1184.

25. **Zhang X, Zhao H, Gao S, Wang WC, Katiyar-Agarwal S, Huang HD, Raikhel N, Jin H.** 2011. *Arabidopsis* Argonaute 2 regulates innate immunity via miRNA393*-mediated silencing of a Golgi-localized SNARE gene, MEMB12. Mol Cell **42:**356–366.

26. **Bhattacharjee S, Zamora A, Azhar MT, Sacco MA, Lambert LH, Moffett P.** 2009. Virus resistance induced by NB-LRR proteins involves Argonaute4-dependent translational control. Plant J **58:**940–951.

27. **Lewsey MG, Carr JP.** 2009. Effects of DICER-like proteins 2, 3 and 4 on cucumber mosaic virus and tobacco mosaic virus infections in salicylic acid-treated plants. J Gen Virol **90:**3010–3014.

28. **Anandalakshmi R, Marathe R, Ge X, Herr JM, Jr., Mau C, Mallory A, Pruss G, Bowman L, Vance VB.** 2000. A calmodulin-related protein that suppresses posttranscriptional gene silencing in plants. Science **290:**142–144.

29. **Ivanov KI, Eskelin K, Basic M, De S, Lohmus A, Varjosalo M, Makinen K.** 2016. Molecular insights into the function of the viral RNA silencing suppressor HCPro. Plant J **85:**30–45.

30. **Pruss G, Ge X, Shi XM, Carrington JC, Vance VB.** 1997. Plant viral synergism: the potyviral genome encodes a broad-range pathogenicity enhancer that transactivates replication of heterologous viruses. Plant Cell **9:**859–868.

31. **Anandalakshmi R, Pruss GJ, Ge X, Marathe R, Mallory AC, Smith TH, Vance VB.** 1998. A viral suppressor of gene silencing in plants. Proc Natl Acad Sci USA **95:**13079–13084.

32. **Nakahara KS, Masuta C, Yamada S, Shimura H, Kashihara Y, Wada TS, Meguro A, Goto K, Tadamura K, Sueda K, Sekiguchi T, Shao J, Itchoda N, Matsumura T, Igarashi M, Ito K, Carthew RW, Uyeda I.** 2012. Tobacco calmodulin-like protein provides secondary defense by

binding to and directing degradation of virus RNA silencing suppressors. Proc Natl Acad Sci USA **109:**10113–10118.

33. **Nakamura H, Shin MR, Fukagawa T, Arita M, Mikami T, Kodama H.** 2014. A tobacco calmodulin-related protein suppresses sense transgene-induced RNA silencing but not inverted repeat-induced RNA silencing. Plant Cell Tiss Org **116:**47–53.

34. **Li F, Huang C, Li Z, Zhou X.** 2014. Suppression of RNA silencing by a plant DNA virus satellite requires a host calmodulin-like protein to repress RDR6 expression. PLoS Pathog **10:**e1003921.

35. **Yong Chung H, Lacatus G, Sunter G.** 2014. Geminivirus AL2 protein induces expression of, and interacts with, a calmodulin-like gene, an endogenous regulator of gene silencing. Virology **460–461:**108–118.

36. **Durrant WE, Dong X.** 2004. Systemic acquired resistance. Annu Rev Phytopathol **42:**185–209.

37. **Liu PP, Bhattacharjee S, Klessig DF, Moffett P.** 2010. Systemic acquired resistance is induced by R gene-mediated responses independent of cell death. Mol Plant Pathol **11:**155–160.

38. **Mishina TE, Zeier J.** 2007. Pathogen-associated molecular pattern recognition rather than development of tissue necrosis contributes to bacterial induction of systemic acquired resistance in Arabidopsis. Plant J **50:**500–513.

39. **Lorrain S, Vailleau F, Balague C, Roby D.** 2003. Lesion mimic mutants: keys for deciphering cell death and defense pathways in plants? Trends Plant Sci **8:**263–271.

40. **Tang X, Xie M, Kim YJ, Zhou J, Klessig DF, Martin GB.** 1999. Overexpression of *Pto* activates defense responses and confers broad resistance. Plant Cell **11:**15–29.

41. **Ohshima M, Itoh H, Matsuoka M, Murakami T, Ohashi Y.** 1990. Analysis of stress-induced or salicylic acid-induced expression of the pathogenesis-related 1a protein gene in transgenic tobacco. Plant Cell **2:**95–106.

42. **Makiyama RK, Fernandes CA, Dreyer TR, Moda BS, Matioli FF, Fontes MR, Maia IG.** 2016. Structural and thermodynamic studies of the tobacco calmodulin-like rgs-CaM protein. Int J Biol Macromol **92:**1288–1297.

43. **Yalpani N, Shulaev V, Raskin I.** 1993. Endogenous salicylic-acid levels

correlate with accumulation of pathogenesis-related proteins and virus-resistance in tobacco. Phytopathology **83:**702−708.

44. **Ji LH, Ding SW.** 2001. The suppressor of transgene RNA silencing encoded by *Cucumber mosaic virus* interferes with salicylic acid-mediated virus resistance. Mol Plant-Microbe Interact **14:**715−724.

45. **Garcia-Ruiz H, Murphy JF.** 2001. Age-related resistance in bell pepper to *Cucumber mosaic virus*. Ann Appl Biol **139:**307−317.

46. **Friedrich L, Lawton K, Ruess W, Masner P, Specker N, Rella MG, Meier B, Dincher S, Staub T, Uknes S, Metraux JP, Kessmann H, Ryals J.** 1996. A benzothiadiazole derivative induces systemic acquired resistance in tobacco. Plant J **10:**61−70.

47. **Gorlach J, Volrath S, Knauf-Beiter G, Hengy G, Beckhove U, Kogel KH, Oostendorp M, Staub T, Ward E, Kessmann H, Ryals J.** 1996. Benzothiadiazole, a novel class of inducers of systemic acquired resistance, activates gene expression and disease resistance in wheat. Plant Cell **8:**629−643.

48. **Lawton KA, Friedrich L, Hunt M, Weymann K, Delaney T, Kessmann H, Staub T, Ryals J.** 1996. Benzothiadiazole induces disease resistance in *Arabidopsis* by activation of the systemic acquired resistance signal transduction pathway. Plant J **10:**71−82.

49. **Anfoka GH.** 2000. Benzo-(1,2,3)-thiadiazole-7-carbothioic acid S-methyl ester induces systemic resistance in tomato (*Lycopersicon esculentum*. Mill cv. Vollendung) to *Cucumber mosaic virus*. Crop Prot **19:**401−405.

50. **Jones JD, Dangl JL.** 2006. The plant immune system. Nature **444:**323–329.

51. **Miyashita Y, Atsumi G, Nakahara KS.** 2016. Trade-offs for viruses in overcoming innate immunities in plants. Mol Plant-Microbe Interact **29:**595−598.

52. **Moffett P.** 2009. Mechanisms of recognition in dominant R gene mediated resistance. Adv Virus Res **75:**1–33.

53. **Zorzatto C, Machado JP, Lopes KV, Nascimento KJ, Pereira WA, Brustolini OJ, Reis PA, Calil IP, Deguchi M, Sachetto-Martins G, Gouveia BC, Loriato VA, Silva MA, Silva FF, Santos AA, Chory J, Fontes EP.** 2015. NIK1-mediated translation suppression functions as a plant antiviral immunity mechanism. Nature **520:**679−682.

54. **Niehl A, Wyrsch I, Boller T, Heinlein M.** 2016. Double-stranded RNAs

induce a pattern-triggered immune signaling pathway in plants. New Phytol **211:**1008−1019.

55. **Takeuchi O, Akira S.** 2010. Pattern recognition receptors and inflammation. Cell **140:**805−820.

56. **Sparrer KM, Gack MU.** 2015. Intracellular detection of viral nucleic acids. Curr Opin Microbiol **26:**1−9.

57. **Cheval C, Aldon D, Galaud JP, Ranty B.** 2013. Calcium/calmodulin-mediated regulation of plant immunity. Biochim Biophys Acta **1833:**1766−1771.

58. **Bender KW, Snedden WA.** 2013. Calmodulin-related proteins step out from the shadow of their namesake. Plant Physiol **163:**486−495.

59. **Zhu X, Dunand C, Snedden W, Galaud JP.** 2015. CaM and CML emergence in the green lineage. Trends Plant Sci **20:**483−489.

60. **Patil A, Nakamura H.** 2006. Disordered domains and high surface charge confer hubs with the ability to interact with multiple proteins in interaction networks. FEBS Lett **580:**2041−2045.

61. **Ren G, Wang X, Chen D, Wang X, Liu X.** 2014. Effects of aphids *Myzus persicae* on the changes of Ca^{2+} and H_2O_2 flux and enzyme activities in tobacco. J PLANT INTERACT **9:**883−888.

62. **Will T, van Bel AJ.** 2006. Physical and chemical interactions between aphids and plants. J Exp Bot **57:**729−737.

63. **Lecourieux D, Ranjeva R, Pugin A.** 2006. Calcium in plant defence-signalling pathways. New Phytol **171:**249−269.

64. **Zhou Y, Frey TK, Yang JJ.** 2009. Viral calciomics: interplays between Ca2+ and virus. Cell Calcium **46:**1−17.

65. **Tsuda K, Mine A, Bethke G, Igarashi D, Botanga CJ, Tsuda Y, Glazebrook J, Sato M, Katagiri F.** 2013. Dual regulation of gene expression mediated by extended MAPK activation and salicylic acid contributes to robust innate immunity in *Arabidopsis thaliana*. PLoS Genet **9:**e1004015.

66. **Chiu MH, Chen IH, Baulcombe DC, Tsai CH.** 2010. The silencing suppressor P25 of *Potato virus X* interacts with Argonaute1 and mediates its degradation through the proteasome pathway. Mol Plant Pathol **11:**641−649.

67. **Pruss GJ, Lawrence CB, Bass T, Li QQ, Bowman LH, Vance V.** 2004. The potyviral suppressor of RNA silencing confers enhanced resistance to multiple pathogens. Virology **320:**107−120.

68. **Lewsey MG, Murphy AM, Maclean D, Dalchau N, Westwood JH, Macaulay K, Bennett MH, Moulin M, Hanke DE, Powell G, Smith AG, Carr JP.** 2010. Disruption of two defensive signaling pathways by a viral RNA silencing suppressor. Mol Plant-Microbe Interact **23:**835−845.

69. **Zhou T, Murphy AM, Lewsey MG, Westwood JH, Zhang HM, Gonzalez I, Canto T, Carr JP.** 2014. Domains of the cucumber mosaic virus 2b silencing suppressor protein affecting inhibition of salicylic acid-induced resistance and priming of salicylic acid accumulation during infection. J Gen Virol **95:**1408−1413.

70. **Li F, Zhao N, Li Z, Xu X, Wang Y, Yang X, Liu SS, Wang A, Zhou X.** 2017. A calmodulin-like protein suppresses RNA silencing and promotes geminivirus infection by degrading SGS3 via the autophagy pathway in *Nicotiana benthamiana*. PLoS Pathog **13:**e1006213.

71. **Huot B, Yao J, Montgomery BL, He SY.** 2014. Growth-defense tradeoffs in plants: a balancing act to optimize fitness. Mol Plant **7:**1267−1287.

72. **Baulcombe DC, Chapman S, Santa Cruz S.** 1995. Jellyfish green fluorescent protein as a reporter for virus infections. Plant J **7:**1045−1053.

73. **Mitsuhara I, Ugaki M, Hirochika H, Ohshima M, Murakami T, Gotoh Y, Katayose Y, Nakamura S, Honkura R, Nishimiya S, Ueno K, Mochizuki A, Tanimoto H, Tsugawa H, Otsuki Y, Ohashi Y.** 1996. Efficient promoter cassettes for enhanced expression of foreign genes in dicotyledonous and monocotyledonous plants. Plant Cell Physiol **37:**49−59.

74. **Matsuo K, Hong JS, Tabayashi N, Ito A, Masuta C, Matsumura T.** 2007. Development of *Cucumber mosaic virus* as a vector modifiable for different host species to produce therapeutic proteins. Planta **225:**277−286.

75. **Kim BM, Suehiro N, Natsuaki T, Inukai T, Masuta C.** 2010. The P3 protein of *Turnip mosaic virus* can alone induce hypersensitive response-like cell death in *Arabidopsis thaliana* carrying *TuNI*. Mol Plant-Microbe Interact **23:**144−152.

76. **Atsumi G, Kagaya U, Kitazawa H, Nakahara KS, Uyeda I.** 2009. Activation of the salicylic acid signaling pathway enhances *Clover yellow*

vein virus virulence in susceptible pea cultivars. Mol Plant-Microbe Interact **22:**166–175.

77. **Yambao MLM, Yagihashi H, Sekiguchi H, Sekiguchi T, Sasaki T, Sato M, Atsumi G, Tacahashi Y, Nakahara KS, Uyeda I.** 2008. Point mutations in helper component protease of clover yellow vein virus are associated with the attenuation of RNA-silencing suppression activity and symptom expression in broad bean. Arch Virol **153:**105−115.

78. **Kanazawa A, Inaba J, Shimura H, Otagaki S, Tsukahara S, Matsuzawa A, Kim BM, Goto K, Masuta C.** 2011. Virus-mediated efficient induction of epigenetic modifications of endogenous genes with phenotypic changes in plants. Plant J **65:**156−168.

Figure Legends

FIG 1 Overexpressed and ectopically expressed rgs-CaM elicits immune responses in tobacco, implying a link between rgs-CaM and salicylic acid signaling. (Ai) Transgenic tobacco plants overexpressing rgs-CaM showed phenotypic characteristics indicating activation of immune responses, such as necrosis and dwarfing, at 7 weeks after sowing of transgenic lines 16 (rgs-CaM16) and 23 (rgs-CaM23). (Aii) Within each of these two transgenic lines, severity of the lesion mimic phenotype was variable. Individual plants from each line are shown in order from mild (1) to severe (6) phenotypes. These individuals were confirmed to have the rgs-CaM transgene by detecting the 35S and rgs-CaM nucleotide sequences by PCR (Aiii). PCR products amplified from the binary vector pBE2113-rgs-CaM, with which tobacco plants were transformed, with the same primer pairs were loaded as a control (lane C). Cell death (B) and generation of reactive oxygen species (ROS) (C) in leaves were compared between transgenic tobacco overexpressing rgs-CaM and wild-type (WT) by Evans blue and 2′,7′-dichlorofluorescein-diacetate (H_2DCF) staining, respectively. BF indicates bright-field images. (Di) Expression of *PR1a*, an indicator of salicylic acid signaling, was

investigated by northern blotting. Samples from seven plants of transgenic line 16 were ordered from left to right in increasing severity of the phenotype. The *PR1a* mRNA level was investigated by northern blotting. Overexpression of rgs-CaM in these plants was confirmed by western blotting for its protein and semi-quantitative RT-PCR (sqRT-PCR) for its mRNA. Wild-type (WT) tobacco was used as a control. (Dii) Transgenic line 23, which overexpressed rgs-CaM and showed a similar phenotype to line 16, was also shown by northern blotting to induce *PR1a* expression; as in the case of line 16, expression varied within the line. Coomassie brilliant blue–stained (CBB) and ethidium bromide–stained (*rRNA*) gels are shown as loading controls.

FIG 2 Defense responses and salicylic acid signaling were induced by transient expression of rgs-CaM. (A) A PVX vector expressing rgs-CaM (PVX-rgs-CaM), a PVX vector expressing the subgenomic RNA containing the rgs-CaM open reading frame without its initiation codon [PVX-rgs-CaM(-atg)], and an empty vector (PVX) were inoculated into wild-type tobacco (cv. Xanthi) plants. Inoculated leaves at 7 days post-inoculation are shown. Their *PR1a* expression was investigated by real-time PCR. The mRNA levels relative to that of mock-inoculated plants are shown in the bar graph (n = 4). Error bars indicate SE. Student's t test was applied to the data and ** indicates P value of <0.01. (B) Protoplasts prepared from wild-type tobacco plants were transfected with expression cassettes with the rgs-CaM cDNA and the modified cDNA without the initiation codon (rgs-CaM(-atg)), and stained with Evans blue. Black bars indicate 50 μm. The cell death rate (Evans blue–stained cells/total cells) is shown in the bar graph (n = 5). Error bars indicate SE. Student's t test was applied to the data and * indicates P value of <0.05 relative to protoplasts without transfection (Cont). (C) When the

940 protoplasts described in (B) were stained with H_2DCF, protoplasts generating ROS were
941 detected among those transfected with the rgs-CaM expression cassette. Among
942 protoplasts transfected with rgs-CaM(-atg) or not transfected (Cont), no H_2DCF signal
943 was detected. BF indicates bright-field images. White bars indicate 10 μm.
944
945 **FIG 3** Susceptibility of rgs-CaM−knockdown tobacco plants to PVX, and salicylic acid
946 signaling in response to PVX infection. (A) PVX was inoculated into rgs-CaM–
947 knockdown (IR-rgs-CaM) and wild-type (WT) tobacco plants. Accumulation of PVX
948 CP and rgs-CaM and of PVX genomic and subgenomic RNAs (*gPVX* and *sgPVX*,
949 respectively) was investigated in the inoculated leaves by western and northern blotting,
950 respectively, at 1 and 3 days post-inoculation (dpi). (B) The same type of inoculation as
951 in (A) was done with more individual plants (n = 8). Accumulation of PVX genomic
952 RNA was measured by real-time PCR using a pair of primers for amplification of a
953 partial cDNA sequence of viral RNA–dependent RNA polymerase (RdRp). Similarly,
954 accumulation of PVX RNAs including both genomic and subgenomic RNAs was
955 measured with a pair of primers for amplification of a partial cDNA of viral coat protein
956 (CP). The levels of *PR1a* (C) and *rgs-CaM* (D) mRNA were investigated by real-time
957 PCR (n = 5). mRNA levels relative to those of mock-inoculated plants are shown. Bars
958 indicate SE. Student's t test was applied to the data and * indicates P values of <0.05.
959 Coomassie brilliant blue–stained (CBB) and ethidium bromide–stained (*rRNA*) gels are
960 shown as loading controls of western and northern blotting, respectively.
961
962 **FIG 4** Implication of rgs-CaM involvement in salicylic acid signaling in response to
963 infection by CMV. CMV-Y (A and B) and CMV lacking 2b (CMVΔ2b) (C and D) were

964 inoculated into wild-type (WT) and rgs-CaM–knockdown (IR-rgs-CaM) tobacco plants
965 and accumulation of CMV CP, 2b and rgs-CaM proteins, CMV genomic and
966 subgenomic RNAs (*gCMV* and *sgCMV*), respectively (A and C), and the *PR1a* and *rgs-*
967 *CaM* mRNAs were investigated (n = 3) as done in Fig. 3 (B and D). (B, exp. 2) The
968 same type of inoculation as in (exp. 1) was done with more individual plants (n = 9) and
969 investigated the *PR1a* mRNA level. Error bars indicate SE. Student's *t* test was applied
970 to the data and * and ** indicate P value of <0.05 and <0.01, respectively. Coomassie
971 brilliant blue–stained (CBB) and ethidium bromide–stained (*rRNA*) gels are shown as
972 loading controls.
973
974 **FIG 5** Model of salicylic acid signaling in response to CMV infection in tobacco plants
975 (A–C) and salicylic acid signaling in response to wounding stress (D, E). (A–C) In this
976 model, rgs-CaM functions as an immune receptor that perceives viral RSS and Ca^{2+}.
977 Tobacco plants induce salicylic acid signaling when rgs-CaM perceives both 2b and
978 Ca^{2+} as CMV infection cues in an inoculated leaf (A) but not when rgs-CaM perceives
979 either 2b or Ca^{2+} alone, e.g., in a non-inoculated upper leaf (B) or in a leaf inoculated
980 with CMV lacking 2b (CMVΔ2b) (C). (D) Transgenic tobacco plants expressing CMV
981 2b and ClYVV HC-Pro were microperforated by bundled pins. Immediately after
982 microperforation, cell death (middle panels) and ROS generation (lower panels) were
983 visualized by staining leaves with Evans blue or H_2DCF, respectively. (E) Expression of
984 *PR1a* was investigated by RT-PCR at different time points after microperforation of
985 tobacco leaves.
986
987 **FIG 6** Induction of salicylic acid signaling in viral RNA silencing suppressor (RSS)-

988 expressing tobacco plants with Ca^{2+} influx. (A) A Ca^{2+} ionophore, A23187 (75 μM),
989 was infiltrated into leaves of wild-type (WT) and transgenic tobacco plants expressing
990 2b, HC-Pro, or CMV CP. At 24 h after infiltration, the mRNA levels of *PR1a* were
991 investigated by northern blotting. + and – indicate infiltration of phosphate buffer (PBS)
992 with and without A23187, respectively. (B) Tobacco leaves were infiltrated with
993 A23187. A23187 was dissolved in PBS at the indicated concentrations and used to
994 infiltrate wild-type (WT) and transgenic tobacco expressing RNA silencing suppressors
995 CMV 2b and ClYVV HC-Pro. Photographs were taken 24 h after infiltration with
996 A23187. (Ci, ii) To test whether *PR1a* induction was dependent on Ca^{2+} influx, EGTA
997 (10 mM) was infiltrated along with A23187. *PR1a* and *rgs-CaM* mRNA levels and rgs-
998 CaM protein levels were investigated by northern and western blotting, respectively, 1
999 and 24 h after infiltration. Coomassie brilliant blue–stained (CBB) and ethidium
1000 bromide–stained (*rRNA*) gels are shown as loading controls.
1001
1002 **FIG 7** *PR1a* induction depends on rgs-CaM. (A) Wild-type (WT) and transgenic
1003 tobacco expressing RNA silencing suppressors CMV 2b and ClYVV HC-Pro were
1004 inoculated with a PVX empty vector (PVX) and a PVX vector expressing the *rgs-CaM*
1005 ORF sequence lacking the initiation codon as a means of inducing VIGS of rgs-CaM
1006 [VIGS(rgs-CaM)]. These inoculated leaves were infiltrated with A23187 (+) orbuffer
1007 alone (−), 3 days after inoculation with PVX. The levels of *PR1a* mRNA, PVX CP, and
1008 *rgs-CaM* mRNA were investigated by northern blotting, western blotting, and semi-
1009 quantitative RT-PCR, respectively, 24 h after infiltration with A23187. Samples were
1010 also prepared from plants that were inoculated with buffer but not infiltrated (Mock)
1011 and those that were neither inoculated nor infiltrated (Cont). (B) WT and transgenic

tobacco plants expressing salicylate hydroxylase (NahG), which antagonizes salicylic acid signaling, were inoculated with PVX and CMVΔ2b and infiltrated with A23187 at 3 days postinoculation. The levels of *PR1a* mRNA and viral CPs were investigated by northern and western blotting, respectively, 24 h after infiltration with A23187. Samples were also prepared from buffer-inoculated plants without infiltration (Mock). Coomassie brilliant blue–stained (CBB) and ethidium bromide–stained (*rRNA*) gels are shown as loading controls.

FIG 8 Enhanced resistance against CMV-Y in SAR-induced tobacco plants depends on rgs-CaM. (Ai) Comparison of symptoms (yellowing) on non-inoculated upper leaves of tobacco plants inoculated with CMV-Y. CMV-Y was inoculated into wild-type (WT) and rgs-CaM–knockdown (IR-rgs-CaM) tobacco plants 7 weeks after sowing. The photograph was taken at 16 days postinoculation (dpi) with CMV-Y. All of the rgs-CaM–knockdown tobacco plants that were inoculated with CMV-Y developed systemic symptoms on their leaves, but wild-type tobacco plants did not express symptoms. (Aii) The difference in susceptibility between wild-type and rgs-CaM−knockdown plants was confirmed by detecting CMV CP in non-inoculated upper leaves of these plants by western blotting. (Aiii) The mRNA level of *rgs-CaM* relative to that of mock-inoculated wild-type plants was investigated by real-time PCR and shown in the bar graph ($n = 3$). Error bars indicate SE. Student's *t* test was applied to the data and * indicates *P* value of <0.05. (Bi) Five days after SAR induction by treatment with benzo-(1,2,3)-thiadiazole-7-carbothioic acid S-methyl ester (BTH), WT and IR-rgs-CaM tobacco plants were inoculated with CMV-Y. Control plants (Cont) were treated with a solution containing 1.4% (vol/vol) acetone and 0.2% Tween-20 (the solution used to dissolve BTH).

1036 Symptoms on upper leaves were photographed 30 dpi. (Bii, iii) CMV CP and 2b
1037 proteins were detected by western blotting. CMV genomic and subgenomic RNAs
1038 (*gCMV* and *sgCMV*, respectively), rgs-CaM and *PR1a* mRNA were detected by
1039 northern blotting. Coomassie brilliant blue–stained (CBB) and ethidium bromide–
1040 stained gels are shown as loading controls. (C) Experiments similar to those shown in
1041 (B) were done with CMVΔ2b. (D) PVX CP accumulation in plants inoculated with
1042 PVX 5 days after BTH treatment. Accumulation of PVX CP was detected in inoculated
1043 and non-inoculated upper leaves by western blotting. CBB-stained gels are shown as
1044 loading controls. Control samples were prepared from buffer-inoculated plants (Mock).
1045
1046 **FIG 9** Degradation of CMV 2b is enhanced by BTH in transgenic BY2 cultured
1047 tobacco cells expressing 2b. Transgenic BY2 cultured cells expressing 2b were treated
1048 with benzo-(1,2,3)-thiadiazole-7-carbothioic acid S-methyl ester (BTH) by adding it
1049 into the medium at a final concentration of 10 μM with or without an inhibitor,
1050 concanamycin A (concA) at 0.1 μM (A) or E64d at 10 μM (B). The CMV 2b and rgs-
1051 CaM proteins were detected by immune staining using specific fluorescent secondary
1052 antibodies 1 h after treatment with BTH with or without an inhibitor. Nuclei were
1053 visualized by DAPI staining. Differential interference contrast (DIC) images are also
1054 shown. White bars indicate 25 μm.
1055
1056 **FIG 10** Reduction of ClYVV HC-Pro accumulation in transgenic tobacco plants
1057 expressing HC-Pro (A) and schematic models of detection and counteraction of viral
1058 RSSs by rgs-CaM (B). (A, left) Four leaves (1–4) of individual transgenic plants
1059 expressing HC-Pro were treated with benzo-(1,2,3)-thiadiazole-7-carbothioic acid S-

methyl ester (BTH). A23187 in PBS was infiltrated into one half of a leaf 1 day after BTH treatment; the other half was infiltrated with buffer (PBS). (A, right) The HC-Pro and rgs-CaM proteins were detected by western blotting. Values under the HC-Pro panel were band intensity of samples from the leaf part infiltrated with A23187 relative to that without A23187 in the same leaf (1–4). (B, left) In normally growing tobacco plants, the rgs-CaM–mediated defense system does not inhibit CMV infection but induces salicylic acid (SA) signaling via perception of CMV 2b and Ca^{2+} as CMV infection cues. (B, center) When the phase of rgs-CaM is changed by SAR induction, subsequent CMV infection is inhibited by rgs-CaM–mediated anti-RSS defense reactions. rgs-CaM directs degradation of RSS (CMV 2b) via autophagy, resulting in reinforcement of antiviral RNA silencing in addition to SA–mediated antiviral immunity. (B, right) When plants are infected with PVX or CMVΔ2b and Ca^{2+} influx is artificially induced with A23187, SA signaling is induced, probably via perception by rgs-CaM of Ca^{2+} and viral proteins other than RSS or host intermediate proteins that are induced by virus infection.

Figure 1

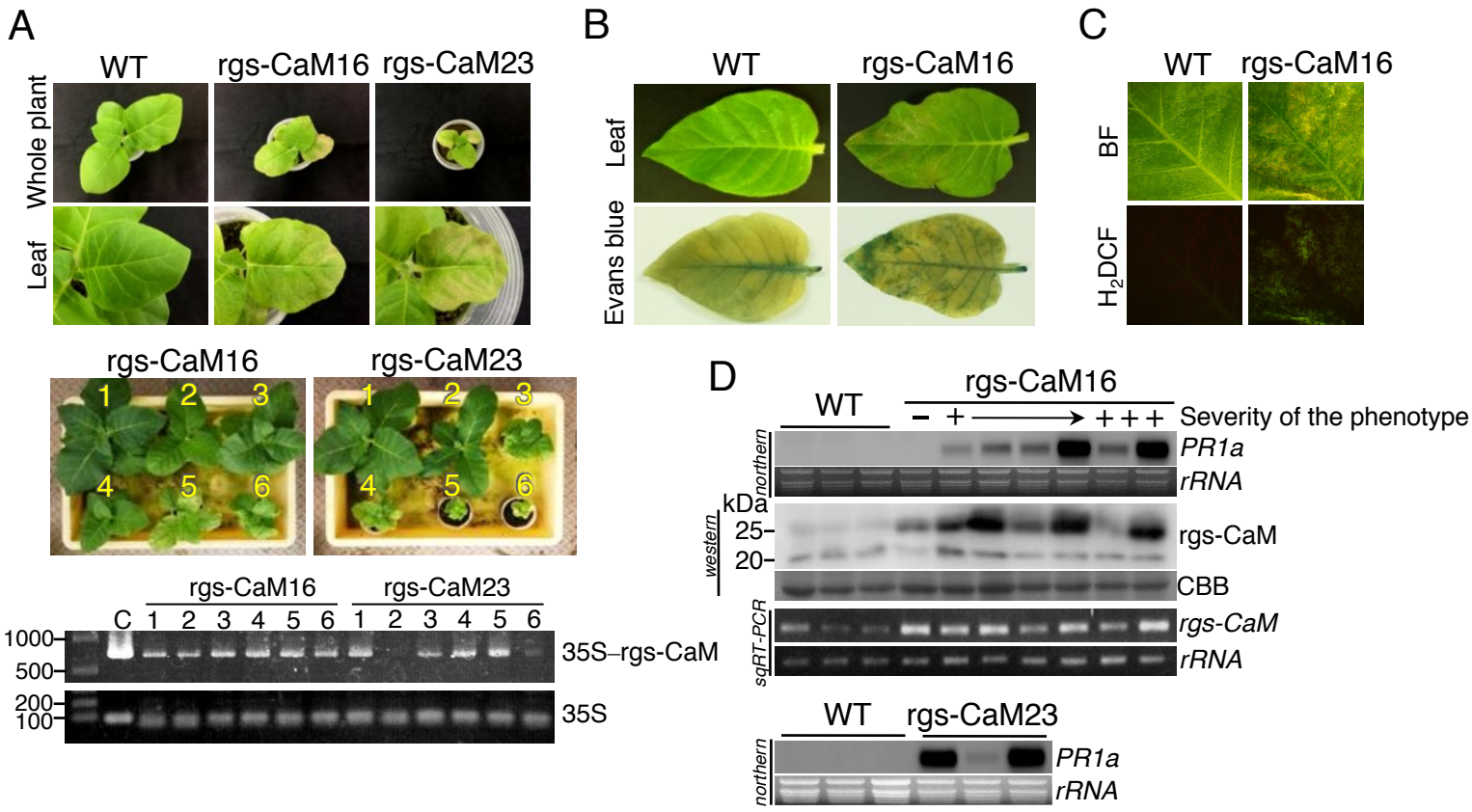
A
WT
rgs-CaM16
rgs-CaM23
Whole plant
Leaf
rgs-CaM16
rgs-CaM23
1 2 3
4 5 6
C 1 2 3 4 5 6 1 2 3 4 5 6
1000
500
200
100
35S–rgs-CaM
35S
B
WT
rgs-CaM16
Leaf
Evans blue
C
WT
rgs-CaM16
BF
H2DCF
D
WT
rgs-CaM16
– + + + +
Severity of the phenotype
northern
PR1a
rRNA
western
kDa
25–
20–
rgs-CaM
CBB
sqRT-PCR
rgs-CaM
rRNA
WT
rgs-CaM23
northern
PR1a
rRNA

Figure 2

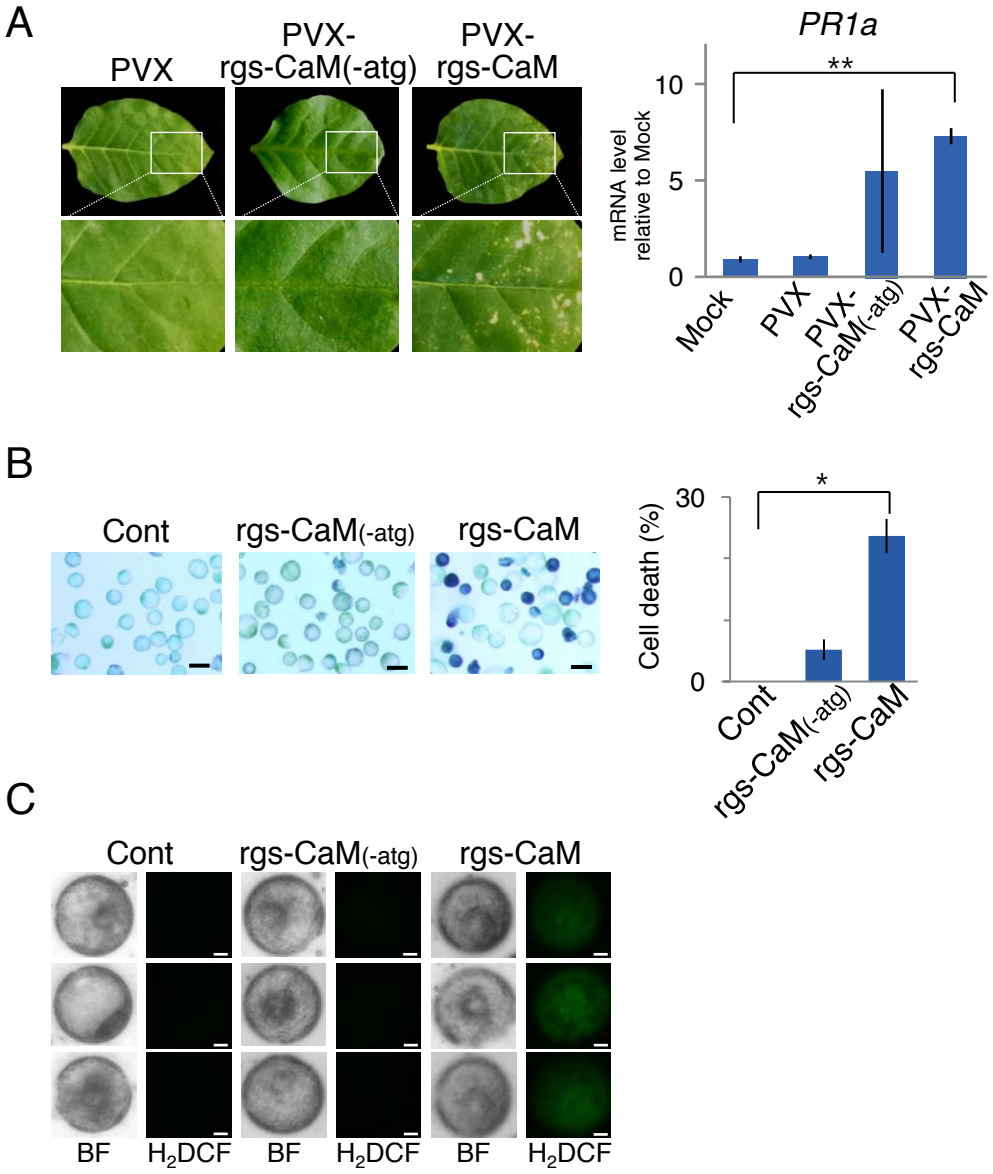
A
PVX
PVX-rgs-CaM(-atg)
PVX-rgs-CaM
PR1a
**
10
5
0
mRNA level relative to Mock
Mock
PVX
PVX-rgs-CaM(-atg)
PVX-rgs-CaM
B
Cont
rgs-CaM(-atg)
rgs-CaM
*
30
0
Cell death (%)
Cont
rgs-CaM(-atg)
rgs-CaM
C
Cont
rgs-CaM(-atg)
rgs-CaM
BF
H2DCF
BF
H2DCF
BF
H2DCF

Figure 3

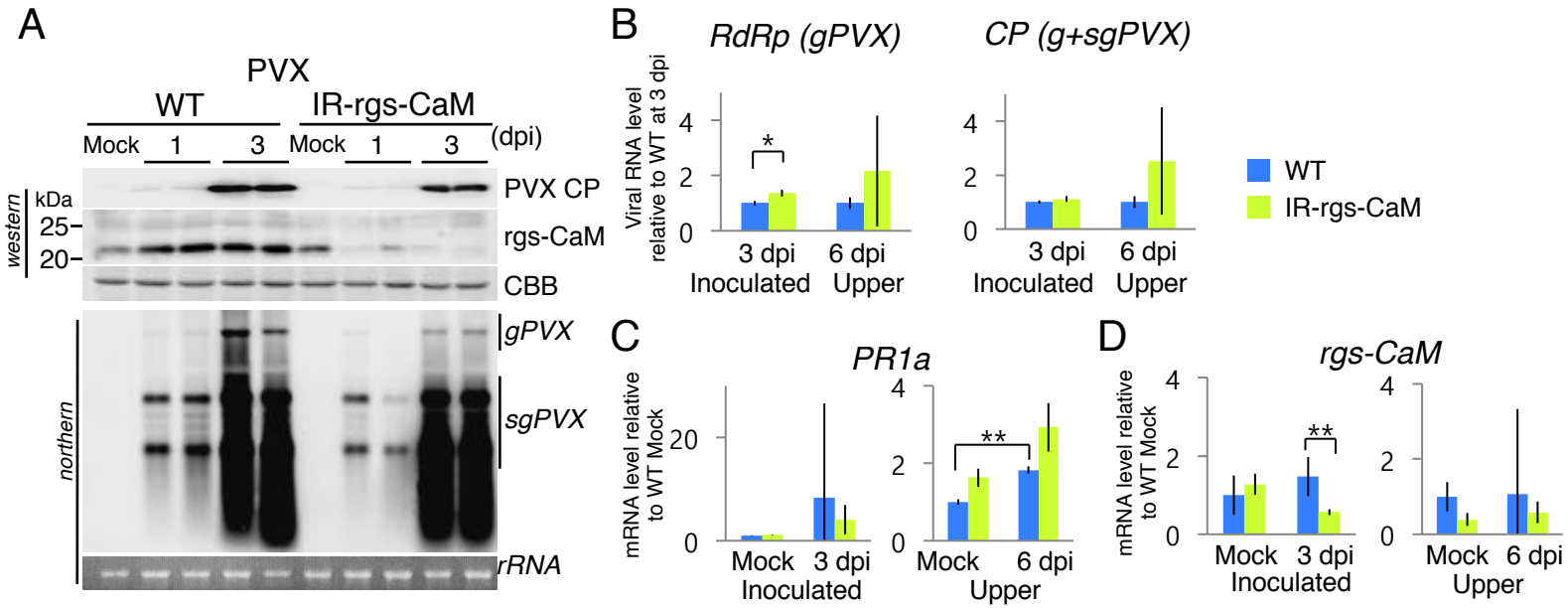
A
PVX
WT
IR-rgs-CaM
Mock 1 3 Mock 1 3 (dpi)
western
kDa
25
20
PVX CP
rgs-CaM
CBB
northern
gPVX
sgPVX
rRNA
B
RdRp (gPVX)
CP (g+sgPVX)
Viral RNA level relative to WT at 3 dpi
3 dpi Inoculated
6 dpi Upper
WT
IR-rgs-CaM
C
PR1a
mRNA level relative to WT Mock
Mock 3 dpi Inoculated
Mock 6 dpi Upper
D
rgs-CaM
Mock 3 dpi Inoculated
Mock 6 dpi Upper

Figure 4

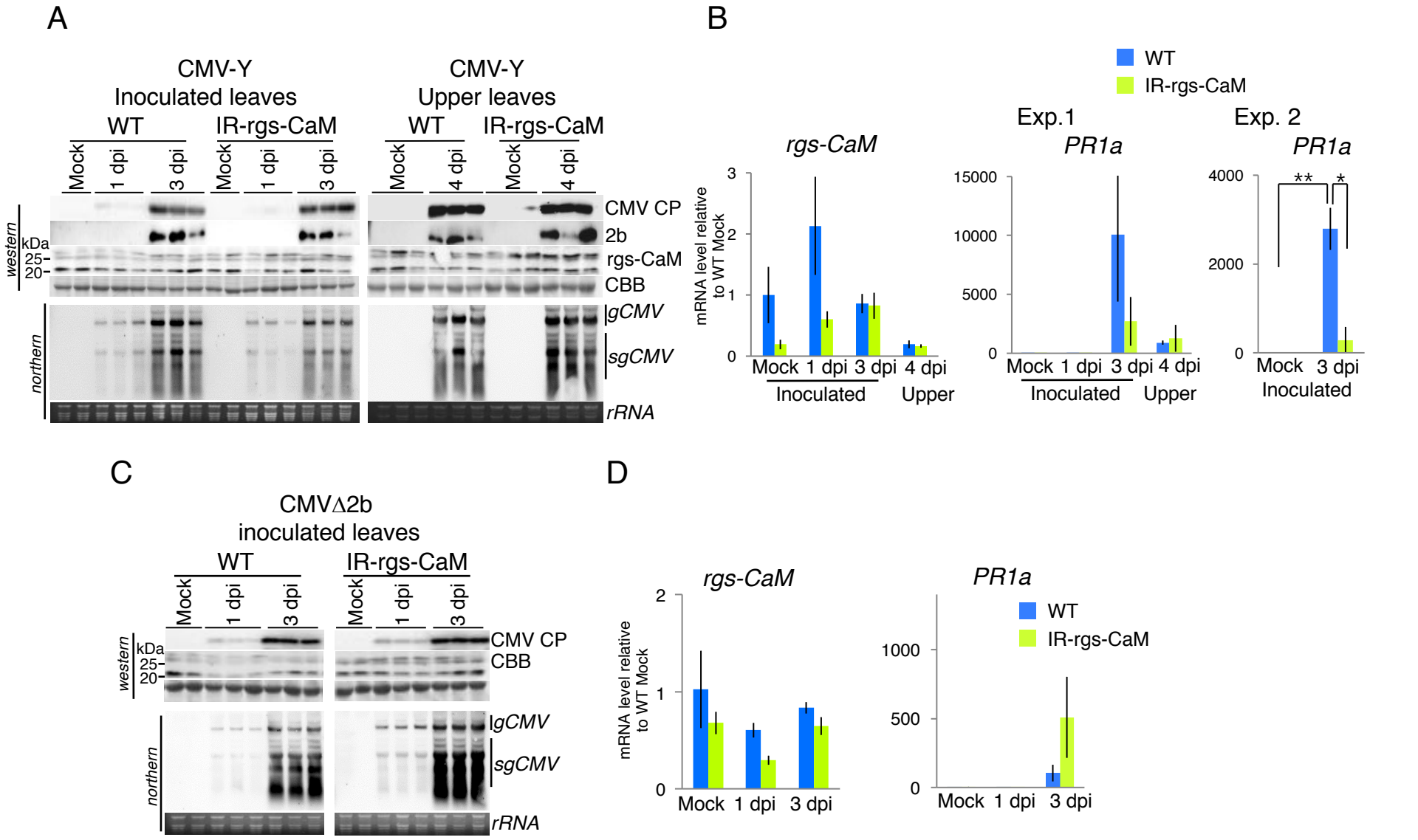
A
CMV-Y
Inoculated leaves
WT
IR-rgs-CaM
Mock
1 dpi
3 dpi
CMV-Y
Upper leaves
4 dpi
western
kDa
25
20
CMV CP
2b
rgs-CaM
CBB
northern
gCMV
sgCMV
rRNA
B
WT
IR-rgs-CaM
rgs-CaM
mRNA level relative to WT Mock
Exp.1
PR1a
Exp. 2
Inoculated
Upper
C
CMVΔ2b
inoculated leaves
D

Figure 5

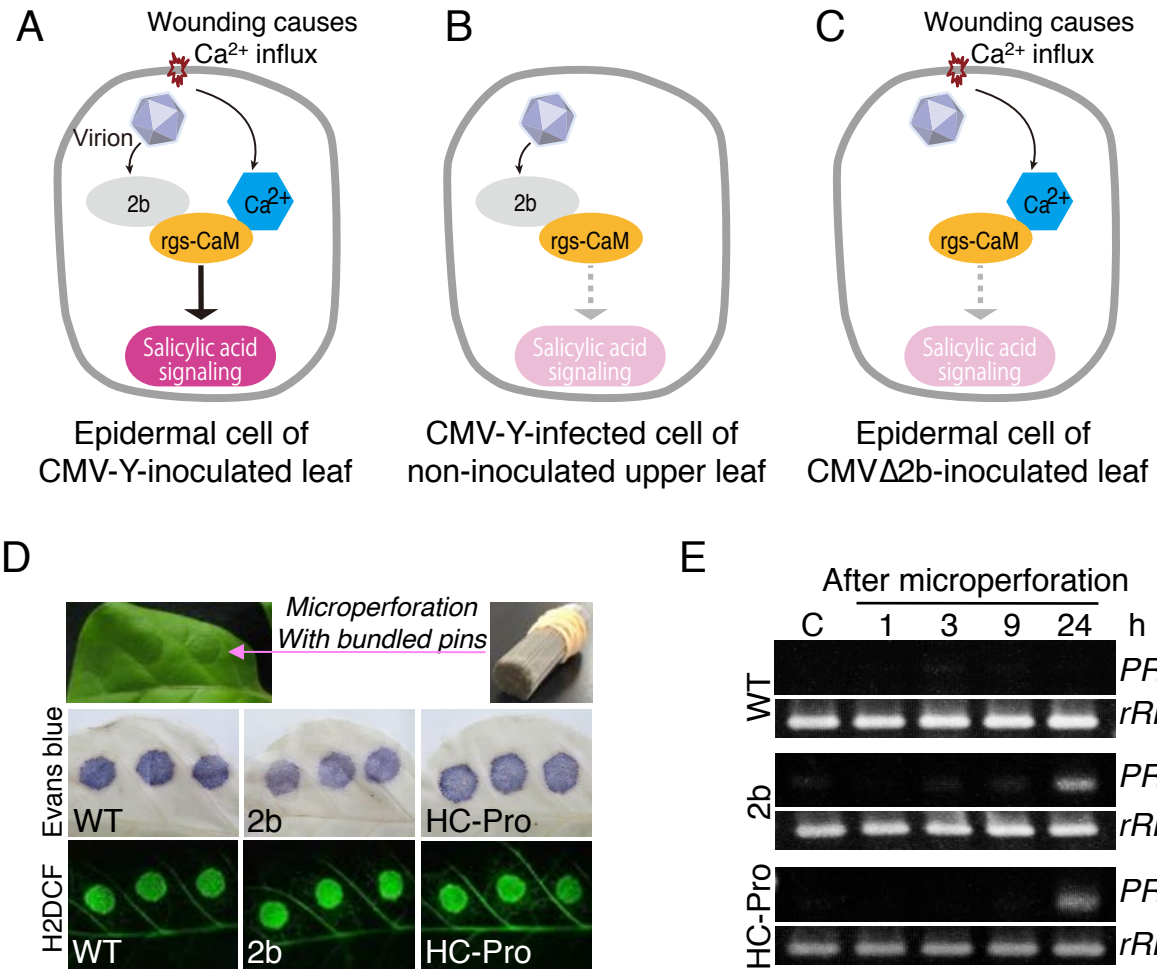
A
Wounding causes
Ca2+ influx
Virion
2b
Ca2+
rgs-CaM
Salicylic acid signaling
Epidermal cell of CMV-Y-inoculated leaf
B
2b
rgs-CaM
Salicylic acid signaling
CMV-Y-infected cell of non-inoculated upper leaf
C
Wounding causes
Ca2+ influx
Ca2+
rgs-CaM
Salicylic acid signaling
Epidermal cell of CMVΔ2b-inoculated leaf
D
Microperforation
With bundled pins
Evans blue
H2DCF
WT
2b
HC-Pro
E
After microperforation
C 1 3 9 24 h
WT
2b
HC-Pro
PR1a
rRNA

Figure 6

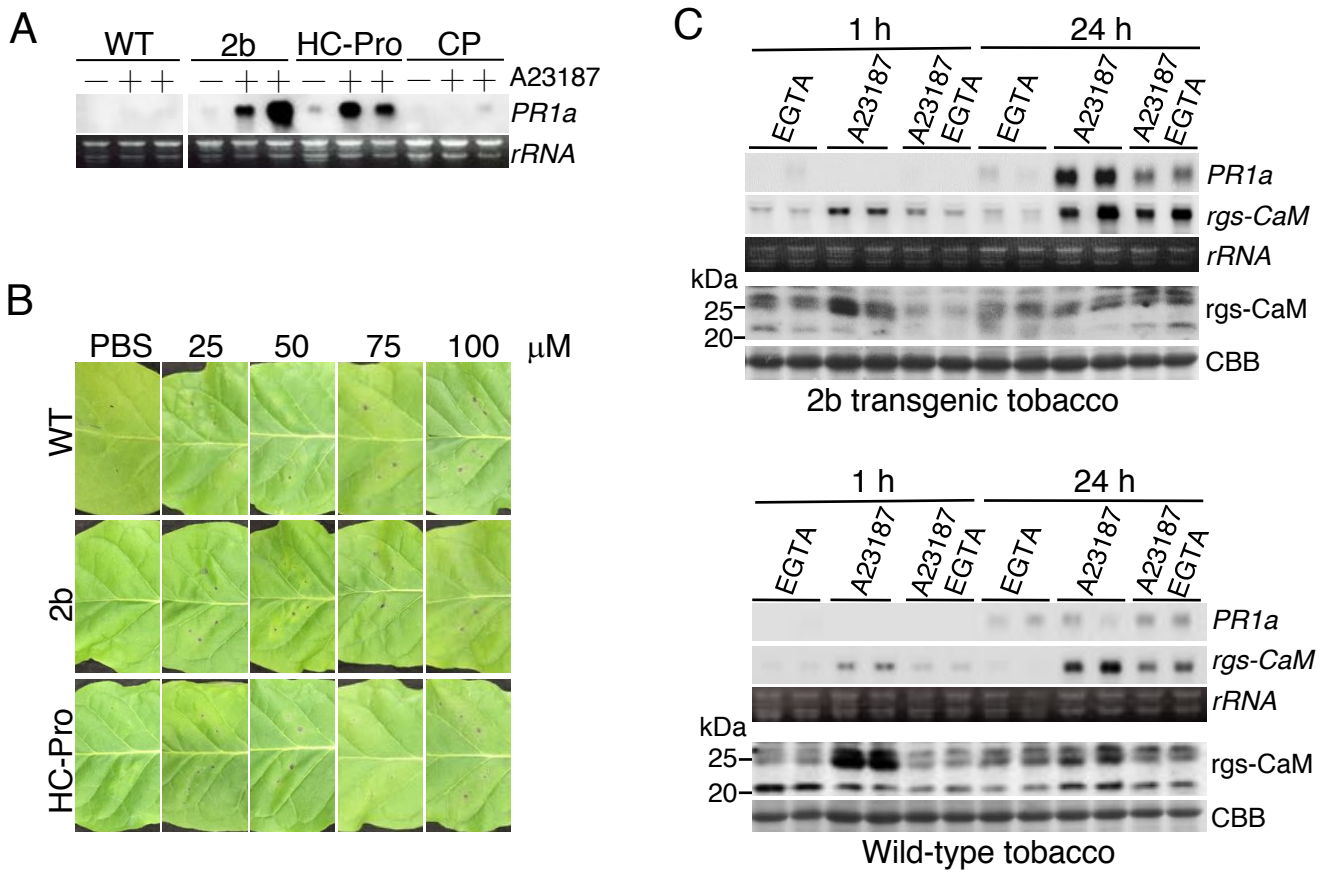
A
WT
2b
HC-Pro
CP
A23187
PR1a
rRNA
B
PBS
25
50
75
100
μM
WT
2b
HC-Pro
C
1 h
24 h
EGTA
A23187
A23187 EGTA
PR1a
rgs-CaM
rRNA
kDa
25
20
rgs-CaM
CBB
2b transgenic tobacco
Wild-type tobacco

Figure 7

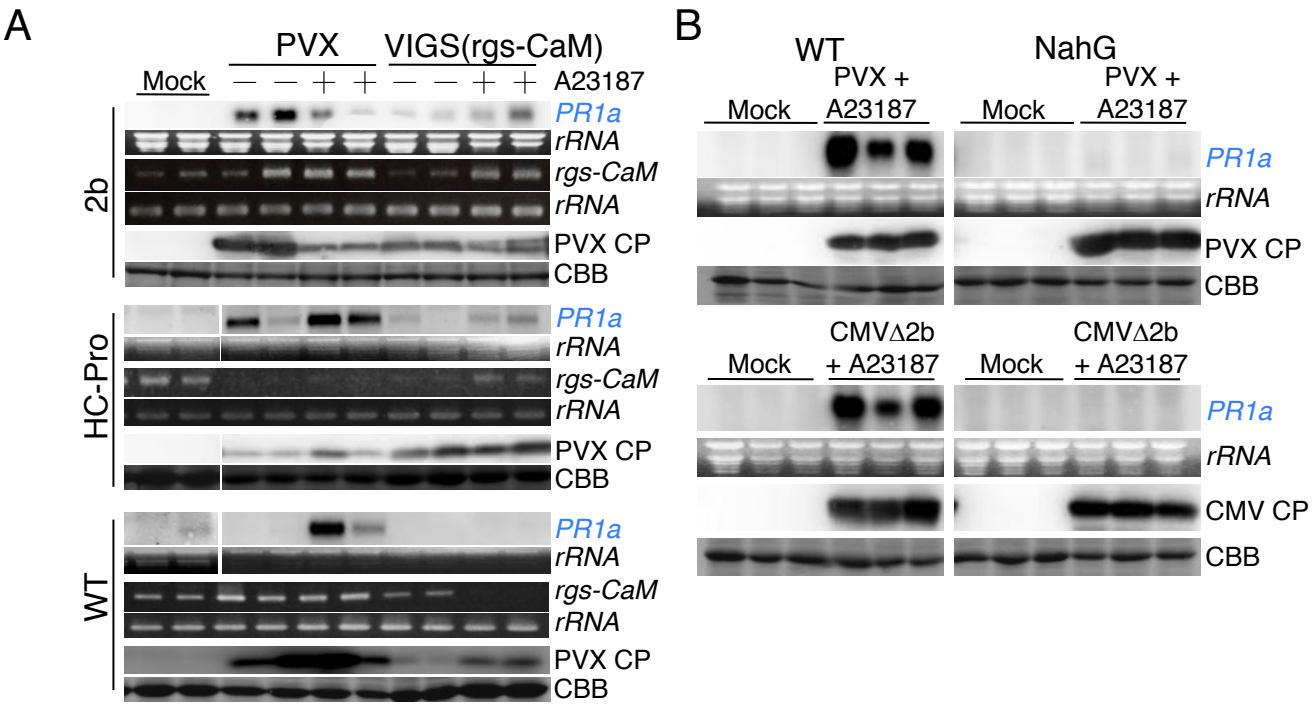
A
PVX
VIGS(rgs-CaM)
Mock
− − + + − − + +
A23187
2b
HC-Pro
WT
PR1a
rRNA
rgs-CaM
rRNA
PVX CP
CBB
B
WT
NahG
Mock
PVX + A23187
CMVΔ2b + A23187
PR1a
rRNA
PVX CP
CMV CP
CBB

Figure 8

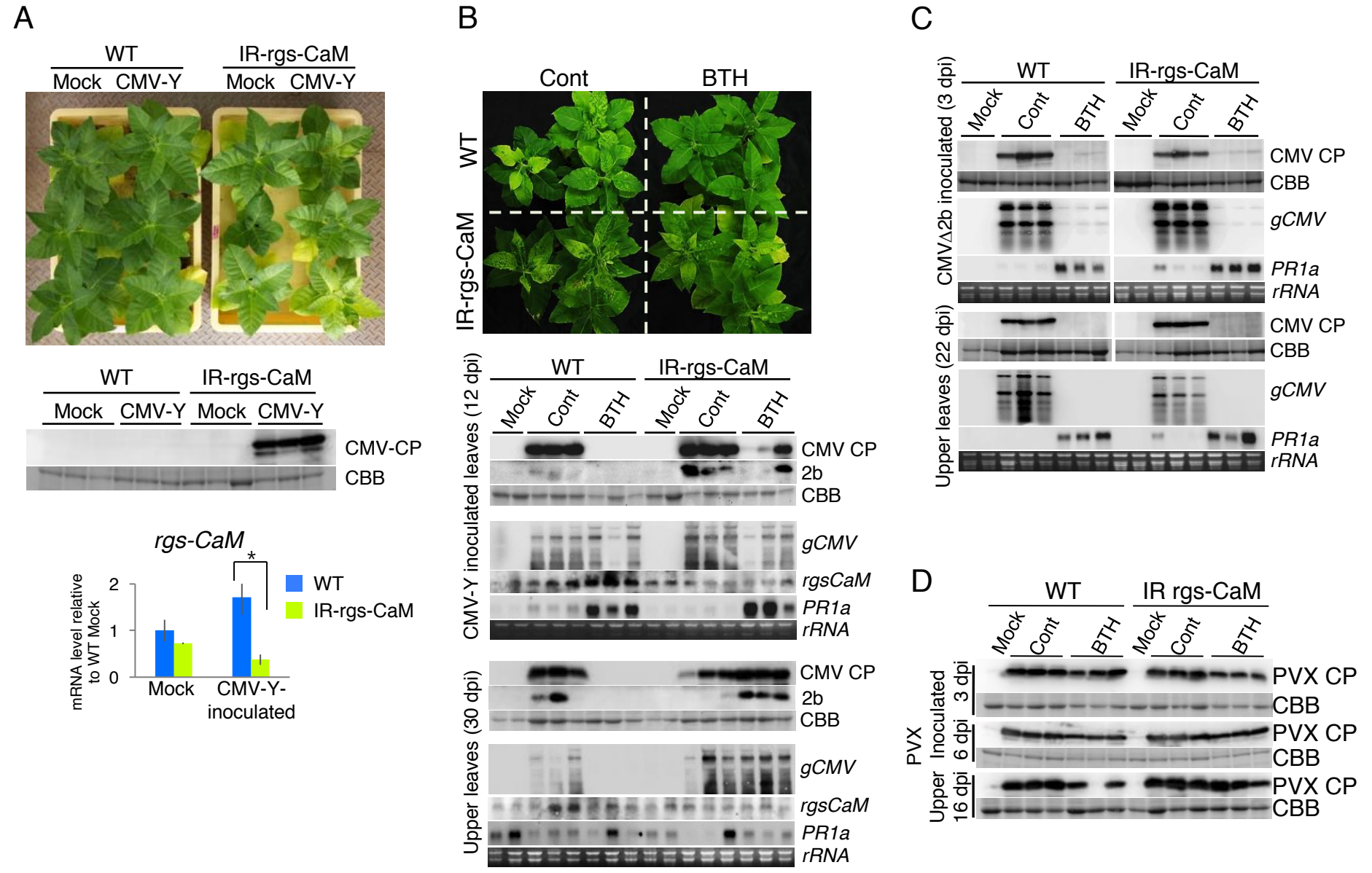
A
WT
IR-rgs-CaM
Mock
CMV-Y
Mock
CMV-Y
WT
IR-rgs-CaM
Mock
CMV-Y
Mock
CMV-Y
CMV-CP
CBB
rgs-CaM
mRNA level relative to WT Mock
2
1
0
*
WT
IR-rgs-CaM
Mock
CMV-Y-inoculated
B
Cont
BTH
WT
IR-rgs-CaM
WT
IR-rgs-CaM
Mock
Cont
BTH
Mock
Cont
BTH
CMV-Y inoculated leaves (12 dpi)
CMV CP
2b
CBB
gCMV
rgsCaM
PR1a
rRNA
Upper leaves (30 dpi)
CMV CP
2b
CBB
gCMV
rgsCaM
PR1a
rRNA
C
WT
IR-rgs-CaM
Mock
Cont
BTH
Mock
Cont
BTH
CMVΔ2b inoculated (3 dpi)
CMV CP
CBB
gCMV
PR1a
rRNA
Upper leaves (22 dpi)
CMV CP
CBB
gCMV
PR1a
rRNA
D
WT
IR rgs-CaM
Mock
Cont
BTH
Mock
Cont
BTH
PVX Inoculated
3 dpi
PVX CP
CBB
6 dpi
PVX CP
CBB
Upper 16 dpi
PVX CP
CBB

Figure 9

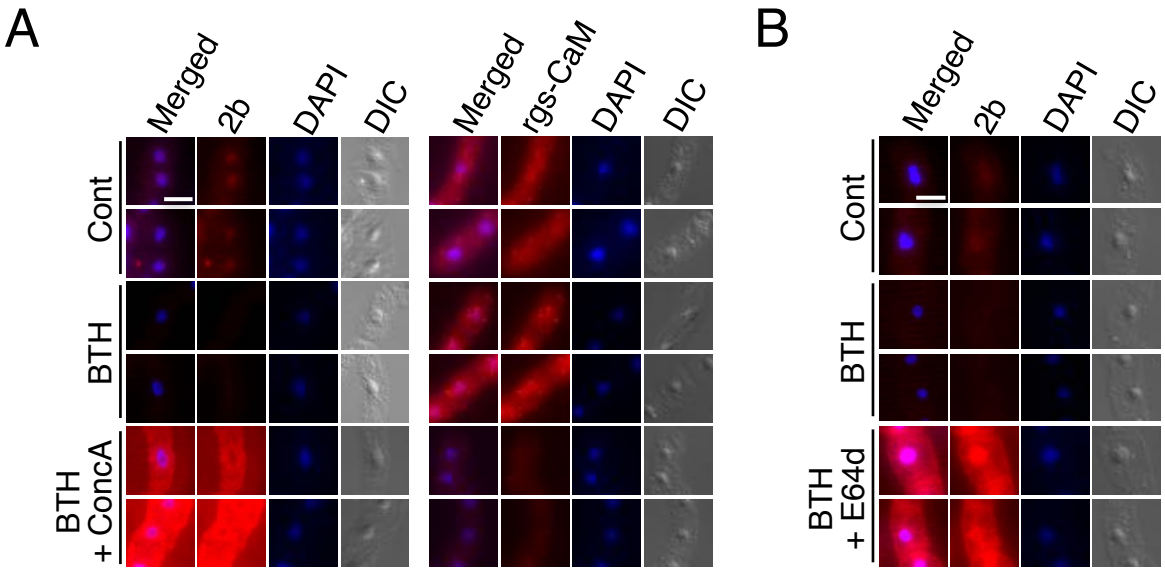
A
Merged
2b
DAPI
DIC
Merged
rgs-CaM
DAPI
DIC
Cont
BTH
BTH
+ ConcA
B
Merged
2b
DAPI
DIC
Cont
BTH
BTH
+ E64d

Figure 10

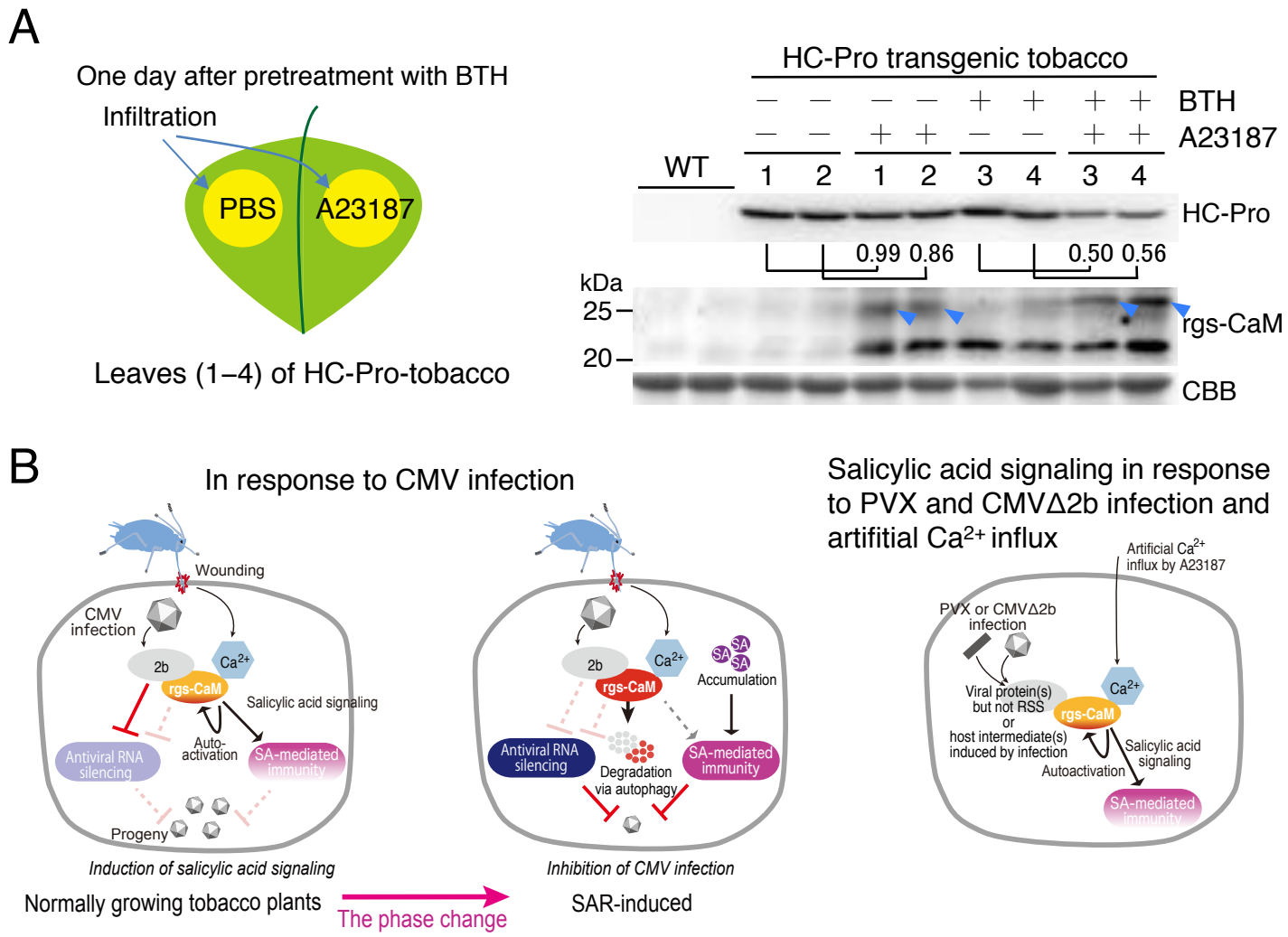
A
One day after pretreatment with BTH
Infiltration
PBS
A23187
Leaves (1–4) of HC-Pro-tobacco
HC-Pro transgenic tobacco
BTH
A23187
WT
1 2 1 2 3 4 3 4
HC-Pro
0.99 0.86
0.50 0.56
kDa
25
20
rgs-CaM
CBB
B
In response to CMV infection
Wounding
CMV infection
2b
Ca2+
rgs-CaM
Salicylic acid signaling
Auto-activation
Antiviral RNA silencing
SA-mediated immunity
Progeny
Induction of salicylic acid signaling
Accumulation
Degradation via autophagy
Inhibition of CMV infection
Normally growing tobacco plants
The phase change
SAR-induced
Salicylic acid signaling in response to PVX and CMVΔ2b infection and artifitial Ca2+ influx
Artificial Ca2+ influx by A23187
PVX or CMVΔ2b infection
Viral protein(s) but not RSS or host intermediate(s) induced by infection
Autoactivation
Salicylic acid signaling

Table 1 Primers used for detection of the viral genomic RNAs and endogenous gene expressions

Gene (accession number)	Primer sequences (5′−3′)
18S rRNA	F CCGTAGTCCCTCTAAGAAGCTG
	R GGTCCAGACATAGTAAGGATTG
rgs-CaM (AF329729)	F TGATAGGAGCATTTGGAATGTATG
	R ACTCATCAAAGTTGAGAACTCCATC
	F ACTATTACTACTGATTATCTTTCGA (semi-Q-PCR)
	R CCCAAGGCCAAAGAATTATGTACA (semi-Q-PCR)
	*F ACTATTACTACTGATTATCTTTCGA
	*R GGGATCCTAATACGACTCACTATAGGGGCAAATGCTCCTATCAATTCACT
CaMV 35S promoter	F CCACTGACGTAAGGGATGACGC
	R GTGTTCTCTCCAAATGAAATGA
PR1a (X06361 Y00707)	F GAAGTGGCGATTTCATGACGGCTG
	R CGAACCGAGTTACGCCAAACCACC
	*F ATGGGATTTGTTCTCTTTTCACAATTGCC
	*R AATTCTAATACGACTCACTATAGGGGAAGGTTCTTGATATCAAGCAG
PVX genomic RNA	*F ATGTCAGCACCAGCTAGCACAACA
	*R AATTCTAATACGACTCACTATAGGGACATTATGGTGGTAGCGTGAC
	F ACCAATCTTTTACAGACTCCACCAC (for RdRp)
	R CTCTAGATCATTAGCCGCTTCAACC (for RdRp)
	F AGGGTCAACTACCTCAACTACCAC (for CP)
	R TCCTTCCAAATAGCCTCAATCTTGC (for CP)
CMV genomic RNA	*F GGCGGGAGCTGAGTTGGCAGTTCTGC
	*R AATTCTAATACGACTCACTATAGGGGGTCTCCTTTTGGAGGCCCCCACGA

* Primers used for making DIG-cRNA probes for northern blotting

F: Sense primer

R: Antisense primer